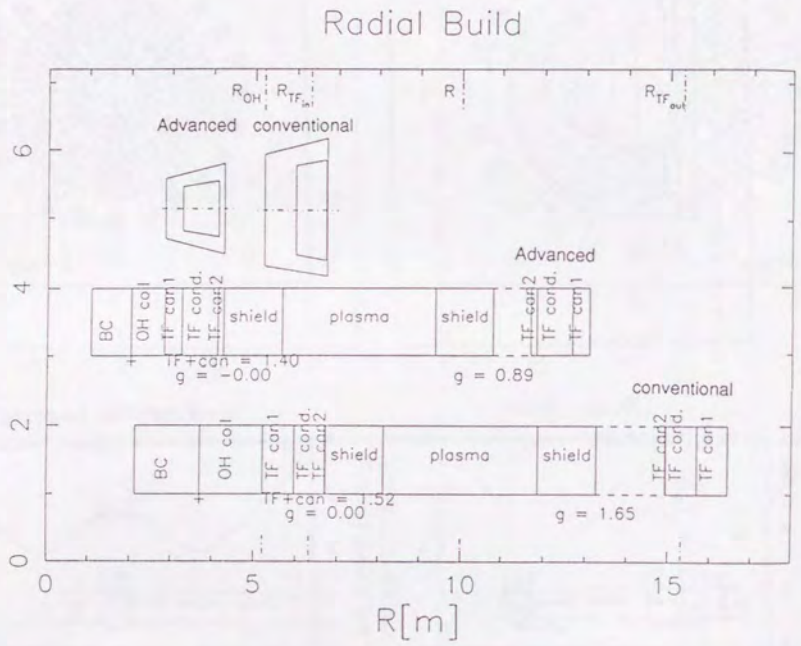

Figure 5.44: Comparison of the radial build between IDLT reactor and Advance IDLT reactor. The cross section of the TF coil is also shown.

Chapter 6

Discussion and conclusion for IDLT reactor

The pulse length of IDLT reactor is very long compared with the dwell time. Therefore, the operation could be called quasi-steady-state operation. At first, the rationale of IDLT reactor is described, then the merits and the demerits of the pulsed reactor and the steady-state reactor are generally listed.

6.1 Rationale of IDLT reactor

The pulsed reactor has two major disadvantage in compared with the steady-state reactor.

- The thermal and the mechanical fatigue of structural materials caused by the repeated operation could be occur.
- The electric power output of pulsed reactor is not constant, the pulsed reactor to the power supply network could not be adaptable.

Such problems of the pulsed reactor are associated with the period of a flattop time of the operation and the operation cycles. These problems are discussed and the rationale of pulsed reactor from the viewpoint of the plant efficiency is also discussed [110].

6.1.1 The occurrence of thermal and mechanical fatigue

One of the most important mission of the next-step DT tokamak experimental reactor is the achievement of the self-ignition and the establishment of the technique for controlling the burning plasma. To achieve the self-ignition, the high field tokamak [111] with the normal conductor and whose pulse length is about 10 seconds has advantageous for its lower construction costs. The reality of the fusion reactor consisting of small high field tokamak operated intermittently is doubtful, because the structural materials cannot stand for the repeated the thermal and the mechanical stress. And the most engineering of small high field tokamak does not link to the engineering of the practical fusion reactor which generate a few GW thermal fusion output. For this reason, the strategy taking the small high field tokamak path is judged to be unfavorable. To demonstrate only some feature of the fusion plant, for example, the engineering, the safety and so on, the construction of a non ignited pilot fusion plant might be taken into the consideration. Different from such the pilot plant concept, the long pulsed tokamak, IDLT reactor, with the superconducting coil system like ITER is discussed in this thesis.

The operation cycle of the pulsed reactor is defined by the permissible stress of the materials standing for the repeated operation. The necessary pulse length depends on the lifetime and the availability of the reactor. Figure 6.1 shows the dependence of the permissible value of the mechanical stress of STARFIRE toroidal coils on the operation cycles calculated as a function of the length of an initial crack on the materials [112]. The direction of the force on the toroidal coil changes as the directions of the plasma current and the vertical field (equilibrium field) coils change. The applied stress on the toroidal coils is smaller when the plasma current flows in both direction alternately compared with the case that if it flows always in one directions. The top horizontal axis of Fig. 6.1 shows the case that the plasma current flows in both direction and the center solenoid coil (CS coil) swing is full. This is the most severe case. The second horizontal axis corresponds

to the case that the plasma current flows in one direction and the CS coil swing is full. The third axis shows the case that the plasma current flows in one direction, and the induction coil swing is half but complemented by the RF current drive. The stress on a vacuum vessel and a shear panel are also considered in the same references. Results of the calculation shows that the materials can put up with about a few ten thousands of repeated operations. Permissible operation cycles can be increased by the additional supporting structure, but it causes cost increase.

If the operation cycles is taken 20,000 $\sim$ 30,000 and to operate the fusion power plant for 30 years with 75% of the availability is assumed, the necessary pulse length is about 7 $\sim$ 10 hours. Plasma major radius which ensures the flux swing of the current transformer necessary for such several hours of the pulse length is about 10 m if the maximum field of 13 T and the flow of the bootstrap current in the plasma are assumed.

The dwell time should be short enough to prevent the significant drop of the temperature in the blanket, the plasma facing components, the turbine generator, and so on, while it should be long enough to perform start up and shut down of the tokamak sufficiently. The start up and shut down time of the typical pulsed reactor is shorter than 10 minutes [98]. Thereby, the pulsed tokamak reactor is operated for about 10 hours and suspended about 10 minutes in one cycle of operation. The availability of such a pulsed reactor is as high as that of the steady-state reactor, because its dwell time is much shorter than the operation time.

6.1.2 Adaptability of the power supply network

The demand for the electric power changes with seasons of the year and with hours on a day. Figure 6.2 shows the typical daily changes of the electric power supplied by the Tokyo Electric Power Company (TEPCO) for a summer day [113]. The peak power supplied on the spring day is about 70% of one of the summer day, while the power supplied during the

night and the power supply patterns are same for both seasons. The difference between supplied powers in the daytime and during the night are quite large, that is ~50 GW versus 25 GW. The base load electric power is supplied by the nuclear power plant, the thermal power plant, and the hydraulic power plant. The fluctuating load is supplied by the thermal power plant and the pumped hydraulic power plant. Especially, the thermal power plant is operated in DSS (Daily Start up and Shut down) mode.

In the above power supply patterns, it should be noticed that the shut down of $1 \sim 2$ GW power plant is nothing but small perturbation and negligible. Actually, the thermal power plant is designed so as that it proofs against the sudden cessation caused by some accident such as thunder, and its performance is examined by the periodic inspection which is carried out once a year. This means that the present power plant system might be applicable to pulsed fusion plant, where shut down takes place regularly once or twice in a day. On that occasion, the valve through which vapor is supplied to the turbine generator closes in about one second after triggering, then the turbine blade house is kept nearly vacuum pressure. Although the rotation speed of the turbine generator drops from 3,000 r.p.m. to 2,000 r.p.m. as the time goes on, the influence of the rotation speed on the restart of that generator is quite small. Hot vapor can be supplied to the turbine blades from another power plants to keep their temperature, if necessary. In the case of pulsed fusion reactor, several kinds of the energy storage system are available [56, 114]. When a 1 GW power plant shutdowns suddenly, the frequency of the power supply network decreases slightly. This frequency drop, however, recovers by the action of an automatic frequency control system. Presently, the thermal power plant with the maximum output power of 1 GW is being operated. The optimum output power of the newly constructed the power plant is about $3 \sim 5\%$ of the maximum network power supply. In the case of Fig. 6.2, the maximum network power is about 50 GW and the optimum output power of the future power plant is around $1 \sim 2$ GW. Thereby, $2 \sim 3$ GW of the output power might be set for the

fusion reactor, if its construction is technically amenable.

From the circumstances discussed above, it is obvious that the IDLT reactor with 1 GW output which is repeatedly operated with the pulse length of several hours and dwell time of about 10 minutes is adaptable to the present power supply network. The loss of the electric power due to the suspension of the IDLT reactor is complemented by another power plant connected to the network, and hence the energy storage system which has been considered so far is not necessary.

6.1.3 Plant efficiency

In this section, a plant efficiency is compared between the pulsed reactor and the steady-state reactor. Fusion reactor is the energy multiplier as shown by the power flow chart in Fig. 6.3, where P_{i} is the input power to the core plasma, P_{f} is the fusion power output from the core plasma which consists of the alpha particle power $P_{\alpha}(= P_{\mathrm{f}}/5)$ in the case of DT reactor, and the total thermal power output from the divertor, the first wall, the blanket, and so forth. Also P_{e}, P_{net}, P_{cir}, P_{d}, and P_{aux} are the gross electrical power output from the turbine generator, the net electrical power from the fusion power plant, the circulation power in the plant, the power for driving the core plasma, and the auxiliary power used for the ancillary devices such as cooling water pumps, respectively. M, η_{d}, η_{e}, and ε are the multiplication factor of a neutron energy in the blanket, the power conversion efficiency of the current drive system and the heating system, the thermal power to the electrical power conversion efficiency of the turbine generator, and the circulation power fraction of the gross electrical power output, respectively.

The energy gain of the core plasma is given by

$$Q = \frac{P_{\mathrm{f}}}{P_{\mathrm{i}}} . \tag{6.1}$$

The plant efficiency η of the power plant is defined as the ratio of the net electrical power output to the thermal power output from the reactor system and calculated from Fig. 6.3

as

$$\eta \equiv \frac{P_{\rm net}}{P_{\rm th}} = \eta_{\rm e} - \frac{P_{\rm cir}}{P_{\rm th}} = \eta_{\rm e} - \frac{1}{Q\eta_{\rm d}} \frac{1}{\left(\frac{1+4M}{5} + \frac{1}{Q}\right)} - \frac{P_{\rm aux}}{P_{\rm th}} . \tag{6.2}$$

The plant efficiency η approaches to $\eta_{\rm e}$ as the efficiency of the power plant increases and the plant efficiency higher than 0.3 is necessary from the economical point of view. From Eq. (6.2) the circulation power sufficiently smaller than the thermal power output is required. The plant efficiencies of the thermal power plant and the nuclear power plant are approximately 0.4 and 0.35. In the case of the fusion power plant, increase of the power plant becomes difficult if high circulation power is required for the plasma current drive or heating.

The energy multiplication factor M of the blanket is $1 \sim 1.4$ for the case of DT fusion power plant. The auxiliary power $P_{\rm aux}$ of the 1 GW net electrical output power plant might be similar to that of the nuclear power output with the same scale, and is estimated to be about 100 MW. Since the thermal power output $P_{\rm th}$ in this case is about 3 GW, then $P_{\rm aux}/P_{\rm th}$ in right hand side of Eq. 6.2 is about 0.03.

In order to achieve high plant efficiency, high values for the energy gain Q and the energy conversion efficiency $\eta_{\rm d}$ are required. For example, in the conceptual design studies of the steady-state tokamak reactors with non-inductive current drive [9, 64, 65], $\eta_{\rm d}$ of $0.5 \sim 0.6$ and Q of $30 \sim 50$ are assumed. While in the case of the inductively driven pulsed reactors, $\eta_{\rm d} > 0.9$ and $Q > 1000$. Although the pulsed reactor looks like advantageous, the difference between plant efficiencies of the steady-state power plant and the pulsed power plant is small, because the plant efficiency approached a constant value if the sufficient amount of Q is attained. Figure 6.4 shows the plant efficiency of fusion reactor, which x axis is shown Q and y axis is shown $\eta_{\rm d}$. In this figure, the region of steady-state reactor shows $Q \sim 50$ and $\eta_{\rm d} \sim 0.5$, on the other hand, the region of pulsed reactor shows $Q \sim 1000$ and $\eta_{\rm d} \sim 0.9$. However, if the current drive efficiency is small in the parameter regime of the burning plasma, the injection of large current drive power is necessary for

driving the same plasma current, and the difference between both types of reactors is not small. In such a case, in the right of Eq. (6.2), the factor $1/Q = P_{\rm d}/P_{\rm f}$ increases and the plant efficiency decreases. The steady-state reactor requires the development of the high efficiency current drive system, but the pulsed reactor does not.

The construction of the pulsed reactor is apparently simple compared with the steady-state reactor, since it does not utilize the complex current drive system with the steady-state operation. Thereby the pulsed reactor is advantageous from the viewpoint of the construction and the economy. In the design study of the steady-state reactor, a highly stable and reliable current drive system is necessarily assumed and the R&D of the current drive system should be completed before the realization of the steady-state fusion reactor. If the plasma volume larger than presently assumed is necessary for the confinement of the burning plasmas, scale up of the current drive system is necessary. The scale of the current drive system approaches that of the tokamak itself. The pulsed tokamak reactor requires also the plasma heating system for ignition at the plasma start up and avoidance of the instability at the plasma shut down. But the steady-state plasma heating is not necessary and the present level of technology is sufficient for these devices.

There are several non-inductive current drive technique, such as the injection of beams of high energy neutral particles and the radio waves at various frequencies, including fast waves, lower hybrid waves, and electron cyclotron waves. The current $I_{\rm CD}$, that can be driven non-inductively is usually determined from the efficiency of the current drive technique, defied as

$$\gamma = \frac{I_{\rm CD} R \langle n_{\rm e} \rangle}{P_{\rm CD}} \ [{\rm A/m^2W}] , \tag{6.3}$$

where $P_{\rm CD}$ is the power launched into the tokamak and available for current drive [115, 116].

Figure 6.5 shows the demonstrated efficiency $\gamma_{\rm D}$ and the extrapolated efficiency $\gamma_{\rm E}$ for each of the current drive techniques and the lines of constant efficiency γ [116]. On the

right-hand ordinate of this figure is shown the launched power required for 18 MA of non-inductive current drive in a tokamak with the major radius R = 8 m. It will be noted that the lower hybrid current drive alone has demonstrated an efficiency as high as the extrapolated efficiency, but only at low density. At the higher density required in a reactor core, only fast wave current drive offers potential, but so far this technique has not been demonstrated.

Concentration of high flux heat load of divertor plate is one of the main issues to be resolved urgently. The inductively driven reactor is advantageous again because the heat load is smaller if the input power to the plasma P_{i} is smaller than the steady-state tokamak reactor.

6.1.4 Summary

IDLT reactor is compared with the steady-state reactor in this section.

- The pulsed reactor has two major problems when compared with the steady-state reactor, that is, thermal and structural fatigue for reputation, and the adjustment between pulsed reactor output and power lines. IDLT reactor avoids these problems by prolonging the operation time to several hours.
- The pulsed reactor might be constructed within the modern technology and does not wait the research and the development of the non-inductive current device.
- The pulsed reactor is advanced from the viewpoint of the plant efficiency. The plant efficiency of the pulsed reactor can be higher than that of the steady-state reactor.

6.2 The merits and the demerits of the pulsed reactor and steady-state reactor

The merits and the demerits of the pulsed reactor and the steady-state reactor are generally listed in this section [117].

6.2.1 The merits and the demerits of the pulsed reactor

The merits of the pulsed reactor are following:

- $Q = P_{\mathrm{thermal}}/P_{\mathrm{injection}}$ is very large, and recirculating power could be small.
- Non-inductive current is still needed, however, its spec can be realized by the state-of-art of technology or a little extrapolation with R&D. There is no need for the steady-state injection.
- The reactor which has the proper performance can be designed with the conventional ITER physics database. If more advanced physics and technology is assumed, the performance of the reactor would make a great step. It is not necessary to innovate on the technology for the pulsed reactor.
- The load-following operation could be possible.

The demerits of the pulsed reactor are following:

- The electronic output from the reactor is varied for the time. It is, however, questionable that it is really the demerit in the power network, such as Japan.
- If the energy reserver for compensating the dwell time is needed, that is disadvantageous to the pulsed reactor from the viewpoint of the cost. The cost of the energy reserver might be larger than the cost of non-inductively current drive system. The reliability of the energy reserver is, however, much larger than that of RF (radio frequency) heating or NBI (neutral beam injection) device, therefore, it could not be selected easily which is better.
- The estimation of the fatigue by the cycle stress is very complicatedly. However, it is possible and it is not fatal for the designing the pulsed reactor.

6.2.2 The merits and the demerits of the steady-state reactor

The merits of the steady-state reactor are following:

- The electrical output is constant for the time.

- The reduction of the number of cyclic stress which introduce the indefiniteness to the reactor design.
- It might be advantage by the disruption control.

The demerits of the steady-state reactor are following:

- The electrical output is constant for the reactor.

  The operation regime is restrict by the parameters for optimizing the efficiency of the non-inductive current drive and the bootstrap current ratio. The load-following operation could not be possible. It might be possible if the efficiency of current drive is improved several times.
- The electrical power which is larger than 10% of electrical output of the reactor should constantly recirculate for RF and/or NBI device. It is the problem on the system reliability although Q value is large or not.

  NBI and RF, however, might be used for the feed-back control of the plasma.
- Q value ($P_{\text{thermal}}/P_{\text{injection}}$) is generally smaller than the pulsed reactor. It cannot follow up although the improvement of the efficiency of the non-inductive current driven would be occur.

6.2.3 Conclusion

It seems to no reason that the steady-state reactor is superior to the pulse reactor by the present condition. Therefore, it must be selected on the cost and the reliability whether the pulsed reactor or steady-state reactor.

To validation of the reliability by the pulsed reactor, it must be shown the stable operation (discharge) by the inductive current. It will be shown that by the ITER. To validation of the reliability by the steady-state reactor, it must be shown the stable continuous operation by the high power non-inductive current drive. It must be shown that by the experiment by using MeV class NBI and/or fast wave current drive. It is also necessary

to prove the stable operation by the current profile control with it.

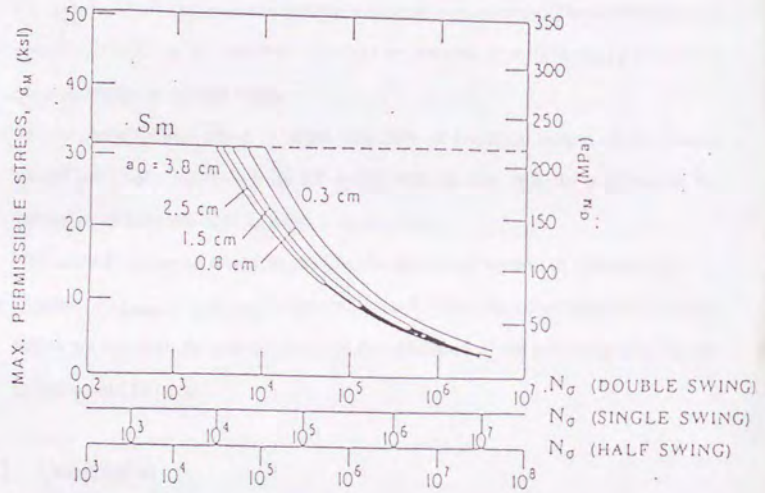

Figure 6.1: Permissible mechanical stress of toroidal coil vs. operation cycles calculated for STARFIRE [112]. Parameters are length of the initial crack. Horizontal axis corresponds to the operation modes of the current transformer, full swing in positive and negative directions (top), full swing in one direction (middle), and half swing in one direction (bottom).

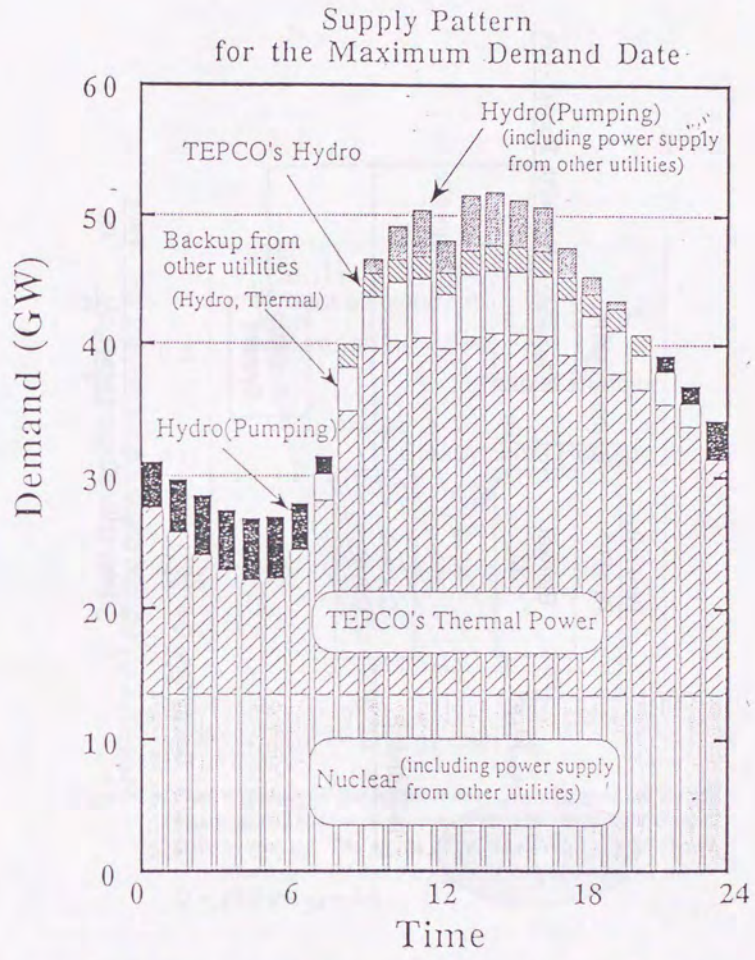

Figure 6.2: Fluctuations of electric power demand [113]. The difference between supplied powers in daytime and during night are quite large, that is ~50 GW versus 25 GW. The shut down of 1 ~ 2 GW power plant is small perturbation and negligible.

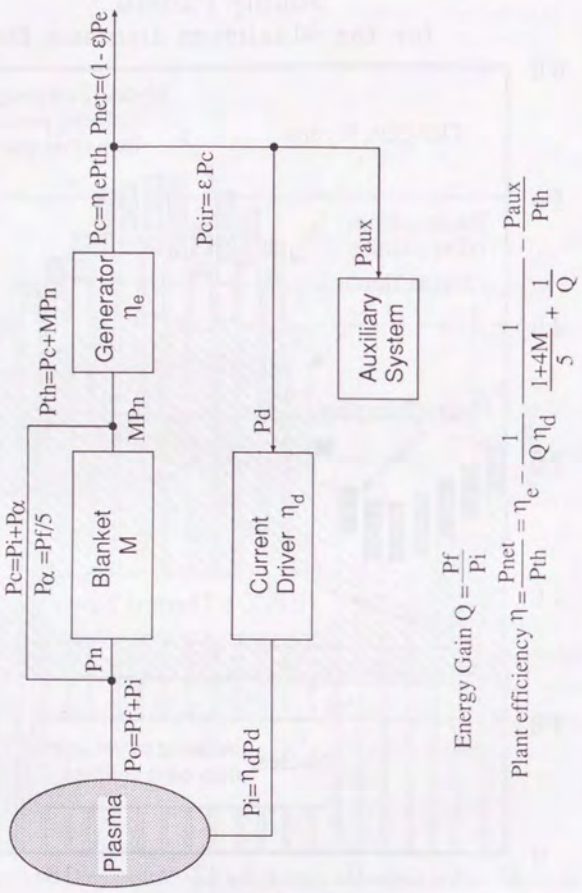

$$\text{Energy Gain } Q = \frac{Pf}{Pi}$$

$$\text{Plant efficiency } \eta = \frac{Pnet}{Pth} = \eta_e \frac{1}{Q\eta_d} \frac{1}{\frac{1+4M}{5} + \frac{1}{Q}} - \frac{Paux}{Pth}$$

Figure 6.3: Power flow char of the fusion power plant [110]. In order to achieve the high plant efficiency, the high values for the energy gain Q and the energy conversion efficiency η_d are required.

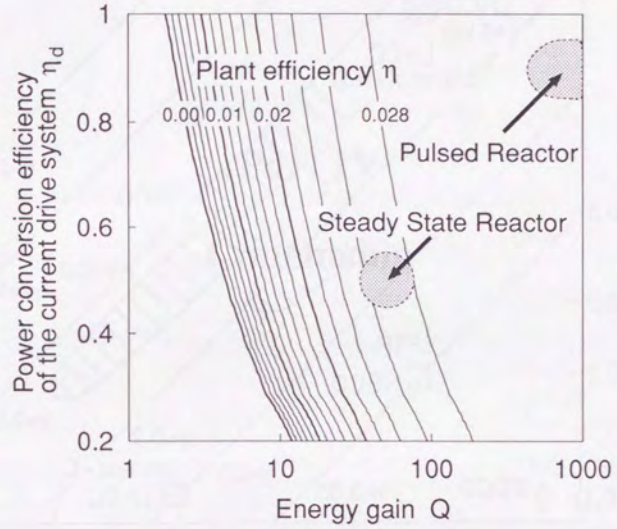

Figure 6.4: Plant efficiency of the fusion reactor. x and y axes are shown energy gain Q and the power conversion efficiency of the current drive system η_d. The region of the steady-state reactor shows $Q \sim 50$ and $\eta_d \sim 0.5$ and the region of the pulsed reactor shows $Q \sim 1000$ and $\eta_d \sim 0.9$.

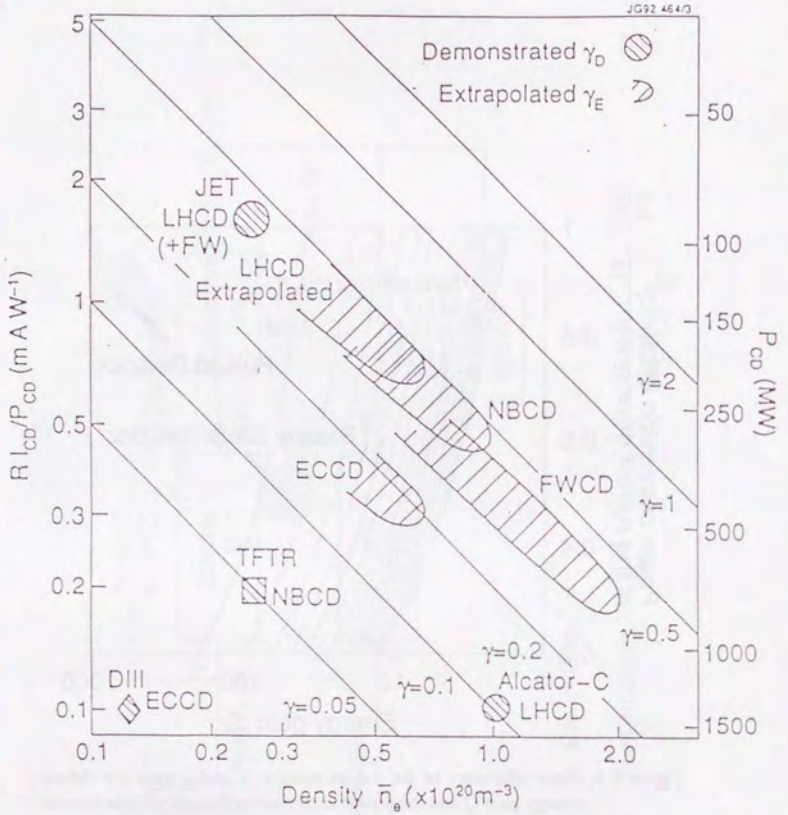

Figure 6.5: Current drive efficiencies, demonstrated and extrapolated, for various techniques of non-inductive current drive [116]. Also shown on the right-hand ordinate is the launched power required for 18 MA of non-inductive current drive in a tokamak with R = 8 m. (LHCD - Lower Hybrid Current Drive; FWCD - Fast Wave Current Drive; NBCD - Neutral Beam Current Drive; ECCD - Electron Cyclotron Drive).

Part IV

Conclusion

Chapter 7

Conclusion

7.1 Discussion

7.1.1 Rough cost estimation by the plasma cross section.

The cross section of ITER (EDA), IDLT Reactors, VNS and Steady-Sate Tokamak Reactor (SSTR) proposed by Japan Atomic Energy Research Institute (JAERI) are shown in Fig. 7.1. Volumetric Neutron Source (VNS) is discussed in Appendix A. The size of plasma cross section has a relation to the cost.

The size of IDLT DEMO reactor is nearly same as that of ITER EDA although the wall loading of DEMO reactor is lower than that of ITER. The cost of IDLT DEMO reactor might be same as ITER.

IDLT commercial reactor is smaller than IDLT DEMO reactor, but is larger than SSTR. The cost of IDLT commercial reactor might be higher than that of SSTR. If advanced physics such as VH-mode is adapted, the major radius is nearly same as SSTR; The cost of Advanced IDLT reactor is approximately same as SSTR.

7.1.2 Route of the fusion developments

The reasonable route for the fusion development with VNS and IDLT reactors is described the following list and Fig. 7.2. This is another way instead of the direct development of the steady-state commercial reactor.

1. Inductively current driven DEMO reactor (low beta/low output fusion power) would be build at first for the early realization because no large R&D is needed. The operating is pulsed operation (*i.e.* IDLT DEMO reactor). The high power output could be operate with the improvement of the material from the results of the material development (*i.e.* ITER, IFMIF, VNS, and so on).
2. The commercial reactor could operate on the extrapolation of the DEMO reactor and it could produce the commercial electrical output (*i.e.* IDLT reactor).
3. After the confirmation of the high performance of the plasma and its safety, the steady-state reactor would be operated (*i.g.* SSTR, ARIES).

This route looks like making a detour, however, the step-by-step developments make the risk low and make the confirmation of the safety more rigid. The total cost of this fusion development route might be lower than that of the direct development route which needs the large R&D such as non-inductive current drive, conceivably.

7.2 Conclusion

- Zero-dimensional system code is developed for checking the parameter fast whether they are valid or not.
- The series of Inductively Driven Long pulsed Tokamak (IDLT) reactor are proposed for early realizing DEMO and the commercial reactor after International Thermonuclear Experimental Reactor (ITER).
- In the IDLT reactor, DEMO reactor and the commercial reactor have been designed with zero-dimensional analysis. The operating scenario of DEMO reactor and the commercial reactor have made from the viewpoint of the plasma equivalence and the poloidal field coil system. The advanced physics make the major radius of the commercial reactor small from 10 m to 7.5 m, although the performance of the reactor is same as the commercial reactor.

In conclusion, the pulsed reactor has been designed as same as the level of the steady-state reactor without the fatal problem.

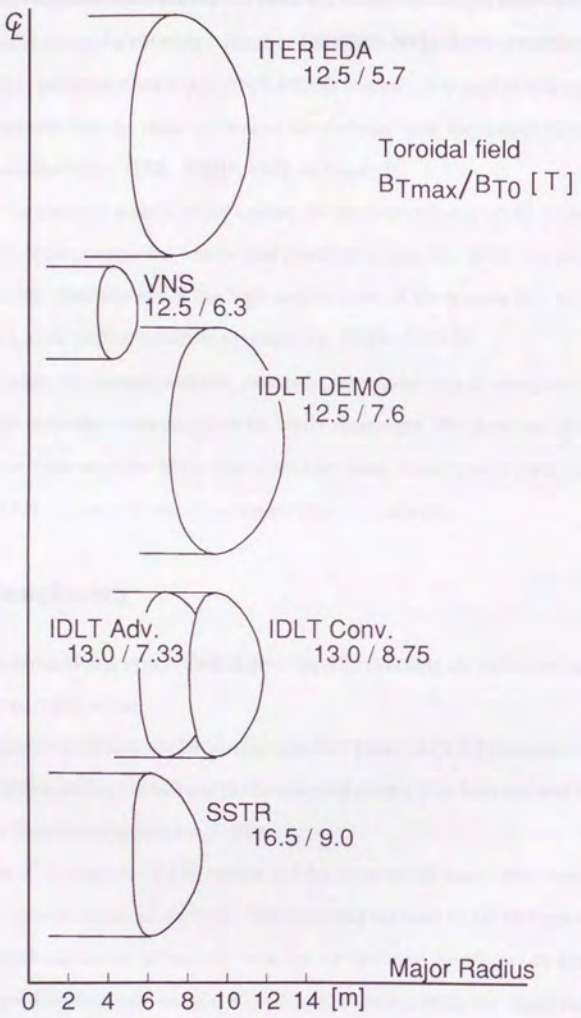

Figure 7.1: Cross section of ITER (EDA), IDLT Reactors, VNS and SSTR.

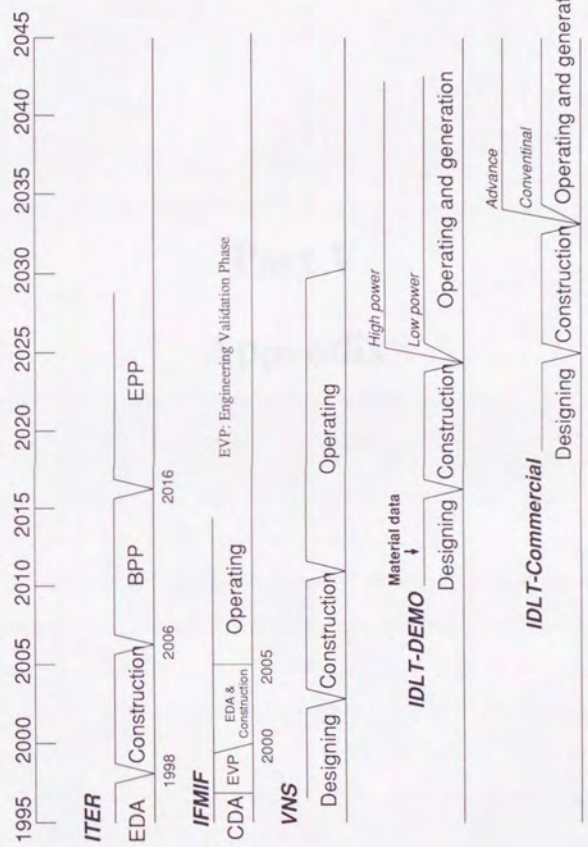

Figure 7.2: Fusion development program.

Part V

Appendix

Appendix A

Volumetric Neutron Source

A.1 Introduction

A.1.1 Requirements of the neutron radiative device

International Thermonuclear Experimental Reactor (ITER) is now in Engineering Design Activity (EDA) and will be started to construct from 1998. The object of ITER is complete the demonstration the scientific feasibility of fusion by achieving controlled and sustained fusion burn for some 1000s and to contribute to the development of technologies needed for a fusion reactor. Basic Performance Phase (BPP) is mainly operated for the plasma physics for the first decade of operation. In the Enhanced Performance Phase (EPP) proceeded BPP, the neutron flux is up to 1 MW/m^2 and total fluence is $1 \sim 3$ MW a/m^2 for test the blanket and the material. This fluence, however, would be too low to choose the adaptive material for DEMO reactor.

To compensate the low neutron flux on ITER, several types of neutron irradiative devices are proposed for testing the material for the next generation reactor; non-neutron test stands, fission reactors, accelerator-based neutron sources, fusion reactors [118].

A.1.2 The merit and the demerit of neutron irradiation devices

Non-neutron test stands

Non-neutron test stands is used in the area of basic property data, single-effect experiments for which the neutron field is not important. It can test the blanket under the high toroidal magnetic field and can investigate the MHD activity of the blanket. The feasibility of the blanket concepts cannot be estimated in the fusion environment. Non-neutron test stands are useful in reducing the large costs and risks associated with future test in the fusion environment.

Fission reactors

Fission reactors provide neutrons in the limited volume and suited to the material experiments. For example, HFIR and EBR-II are in the USA, JRR-2 is in Japan. The merit for using fission reactors is reliability. Most serious demerit is the small test volume, there is no fission reactor operating now in the world that can provide a test location with 15 cm to 1 MWa/m^2. Non-fusion environment make the experiments such as the magnetic force and the mechanical force very difficult. Another problem is the difference between fission reactor and fusion reactor by the neutron and secondary γ-ray spectra. The material test needs the 14 MeV neutron to simulate the fusion environment, however, the fission reactors can produce only under 2 MeV neutrons. Fission reactors is useful, for example, a unit release behavior.

Accelerator-based neutron sources

Accelerator-based neutron sources produce 14 MeV neutrons in a small volume that they are normally called "point neutron source". The neutron spectra is correct fusion spectra but very low neutron flux. An example DT point neutron source is the FNS facility in Japan [119]. FNS provides a neutron flux several orders of magnitude lower the present

plasma physics device. The neutron yield is 5×10^{12} n/s, TFTR could provide 2×10^{18} neutron per shot.

Other proposal for accelerator-based neutron sources have been made. the most prominent is a proposal for a (D, Li) source which neutrons are produces by bombarding a flowing lithium target with high energy (about 40 MeV) deuterium. One of them is the International Fusion Material Irradiation Facility (IFMIF) [120]. IFMIF is now studied by an international activity under the auspices of the International Energy Agency (IEA). The studies indicate a volume of about 0.5 L is required in a region producing a 2 MW/m^2 neutron flux or greater and a fraction of this volume, about 0.1 L would be available at a 5 MW/m^2 neutron flux. But these volume is not enough to test the fusion reactor module, such as the blanket.

Fusion reactors

Fusion plasma devices produce 14 MeV D-T fusion neutrons, and the irradiation of the large size test material is possible, so called "volumetric neutron source" (VNS). There are many type of VNS, mirror confinement [121], Z-pinch, plasma focus, reversal-field-pinch, ultra-low-q tokamak [122, 123], spherical torus [124] and two component-torus (TCT) plasmas. These have been proposed and feasibility study has been carried out. The R&D issues on plasma physics and fusion technology, however, should be solved for these devices.

A Tokamak device is a prominent candidate for VNS. The plasma physics of tokamak plasma has been studied during the past decades, we now can extrapolate the database to an ignition device regime with high reliability such as ITER. In the past, the neutron source based on tokamak plasma [125] was proposed where plasma parameters extrapolated from the database of the supershot in the Tokamak Fusion Test Reactor (TFTR) [126]. Recently, two distinct designs have been promoted; one is a small device ($R < 2$m) with copper con-

ductor, and another is a medium-size device ($R < 4$m) with a super-conductor [127, 128]. In the former case the tritium consumption is $1 \sim 2$ kg/year, which could be supplied by external tritium facility. The demand power for normal conductor, however, is estimated to be a few hundreds MW. In the latter case the plasma volume is so large that the breeding blanket is required for the tritium of a few kg or more. This situation for the necessity of breeding blanket is quite similar to that of ITER-EPP.

A.1.3 Design principle for VNS

A VNS designed in this thesis has some criteria [129, 130]. It is based on the tokamak plasma, aspect ratio A is to be $2.5 \sim 7$ for the high reliability. The physical and the engineering parameters employs in the ITER Conceptual Design Activity (CDA), Engineering Design Activity (EDA) design and its reasonable extension. The plasma size is smaller than ignition device because the plasma is subignited and continuous heated by the auxiliary heating power. Auxiliary heating power is also used current drive power. The advanced plasma study also can be done with this auxiliary heating power by the current profile control such as the reversed shear profile.

The flux of VNS might be larger than ~ 1 MW/m^2. The flux of DEMO reactor is $2 \sim 3$ MW/m^2, the fluence for test material needs $\sim$ 10 MW·yr/m^2 or more during the plant life. Therefore, the steady-state neutron source of $0.5 \sim 1$ MW/m^2 might be a minimum criterion for the material test facility.

Main parameters of VNS are listed in Table A.1. Main parameters are determined from the physical restriction and the engineering restriction. For example, Troyon factor $g = 3$ is decide from the physical consideration. Albeit it is not listed in this table, the shield thickness of 1.4 m is come from the engineering consideration [129].

The time schedule of VNS with ITER, IFMIF and IDLT reactor series is shown in Fig. A.1. DEMO reactor and the commercial reactor would use the material date from ITER, IFMIF and VNS. If the material endured high neutron load will be found, IDLT DEMO reactor could operate the high power output.

A.2 0D system analysis

0D system code is used to exam the main parameter of VNS listed in Table A.1. The code validates the parameters from the engineering aspect especially the poloidal field (PF) coil position and the toroidal field (TF) coil position. The results are shown in Fig. A.2.

The average neutron load is 0.77 MW/m^2 and the maximum neutron load is 1.14 MW/m^2, which is larger than criterial value of 1.0 MW/m^2.

The position of the outer TF leg is rather wide because of keeping the distance between the outer leg and neutral beam injection (NBI) device to protect the radiation damage. Therefore, the TF coil ripple on the plasma surface is very small of 0.2%. The number of TF coil is 16.

The plasma is single null configuration for extending the divertor region. The axis of plasma is moved upward about 1.0 m from the equatorial plan.

A.3 Plasma equilibrium

Plasma equilibrium is calculated by EQUCIR code. PF coils are stand outside of TF coil for easy construction and maintenance. The position of PF coil is decide to be the lowest stored energy of PF coils.

First, the winding method for center solenoid (CS) coil is selected whether pancake winding or layer winding. Second, the power supply for PF coil is determined from the calculation of sequence of the plasma equilibrium on the step time of the ramp-up phase.

A.3.1 Winding method for center solenoid coil

The select of the CS coil winding method is analyzed at the flux supplied by the PF coil is zero. Figure A.3 shows the plasma equilibrium of VNS in two CS coil winding method. The stored energy of layer winding is much larger than that of pancake winding. The divertor coil also large in the case of layer winding. Then pancake winding is selected for the CS coil winding method.

Previous IDLT DEMO and commercial reactor are select the layer winding. The key might be a ratio of the CS coil's height and radius. The difference of the stored energy between the pancake winding and the layer winding would be larger as the ratio is larger. To explicate this relation, more calculations are needed.

A.3.2 Power supply for poloidal field coil

The PF coil of VNS is the superconducting coil, the maximum power demand is occurred in the ramp-up phase described in the previous IDLT section.

It might not necessary to shorten the dwell time as commercial reactor, because VNS is a steady-state reactor. We choose 25 minutes (1500 seconds) for the ramp-up phase. The variation of the plasma parameter as the function of time is shown in Fig. A.4. The plasma is limiter configuration for first 500 seconds, and it is change to the single null configuration after 500 second and keep it to flat-top. The series of growing the plasma cross section is shown in Fig. A.5. The plasma is reached steady state at 1500 second.

The power supply for PF coil is calculated from the PF coil current at each time step and the mutual inductance between the coils and the plasma. In the case of Fig.A.4, the maximum demand power for PF coil is 280 MW.

A.4 MHD analysis

Magnetohydrodynamics (MHD) instability [131, 132] is checked on the VNS plasma by the simulation codes. Kinetic instability and ballooning mode is investigated in this section. We can find a pressure profile which has the critical toroidal beta β_t, that is the maximum β_t which stables for these instability.

The pressure profile is realized by the non-inductive current drive such as neutron beam injection (NBI) and lower hybrid resonant frequency (LHRF) heating. VNS do not use inductively current drive, the plasma current consists of the non-inductive current and the bootstrap current [8]. The aimed pressure profile is accomplished by the non-inductive current drive which is adjusted by the results of the simulation.

Recently, the plasma with non-monotonic q profile, so called "reversed shear profile" is pointed out because of the desirable confinement [133]. VNS could give the higher neutron flux to the test material when the plasma is reversed shear profile. The reversed shear profile is also simulated in this section.

A.4.1 Simulation code

To find out the critical beta, three simulation codes, EQLAUS, ERATO [44, 45], and DRIVER [47] are used. The simulation here is self-consistent by these codes.

First, an MHD equilibrium marginally stable against ballooning, kink, and Mercier modes is determined by iterative calculations with EQLAUS and ERATO code. Then, the optimized current profile $j(\psi)$, where ψ is the magnetic flux function, the pressure profile $p(\psi)$ for the beta limit, and other equilibrium data are transferred to the neutral beam current drive (NBCD) analysis code DRIVER. After this, the beam power distribution in the beam transmission line and the fuel ion density profile are determined by iterative calculations of the current drive and the total pressure. In this way it is ensured that $j(\psi)$ and $p(\psi)$, which is composed of thermal, beam and alpha particle pressure, are

exactly same as those used in the EQLAUS/ERATO calculations. The controllability of the flexible current profile by NBCD make such a current profile tailoring possible. A beam design which is optimized to sustain the critical beta equilibrium is obtained with this method, and the optimized solution gives various figure of merits such as the current drive efficiency, the shinethrough, Q-value and others.

DRIVER code is also includes in addition a self-consistent global power, momentum balance and bootstrap current calculations [48]. The fast ion Fokker-Planck code is bounce-average type. Therefore, the code fully includes the toroidal effect on the fast ion current as well as on the beam-induced electron current. The beam deposition is calculated by a three-dimensional model, which includes the exact calculation of the beam stopping cross-section enhancement due to the multi-step ionization.

A.4.2 Reversed shear mode

The ordinary tokamak's q profile is monotonical increase as the plasma minor radius. It is come from the ohmic current mainly flows the center region of the plasma. Magnetic shear is defined as $s = dq/dr$, the ordinary tokamak's shear is positive all of the part and $q_{\min}$ is located the magnetic axis of the plasma.

The bootstrap current is flowed the periphery of the plasma and the off-axis non-inductive current drive technique is use to flow the periphery current. $q_{\min}$ is moved from the axis to the periphery. Therefore, the shear becomes negative in the central part, so called "reversed shear profile". Figure A.6 shows the ordinary q profile and the reversed shear mode's q profile.

Good plasma confinement is produced by reversed shear mode [134]. It has been known for some time that reversed shear gives robust stability against high-n ballooning modes [135, 136]. If one thinks of the basic interchange drive as being tied the radial derivative of the flux-tube volume, $\int dl/B$, then the source of the ballooning drive along the outer

mid-plane of the tokamak can be seen to come simply from dB/dR. However, if the magnetic shear is negative, then the flux tube length, $\int dl$, shortens with increasing R, which is stabilizing. The ultimate result is that ballooning modes are stable at any β, for the region that magnetic shear is negative.

Joint European Torus (JET) results with the pellet injection starting 1988 provided some of the first experimental indication of effects associated with reversal shear [137]. When pellets were injected early in the discharge, very high pressure gradients were observed in the core of the plasma as the center of the plasma re-heated. Core thermal confinement improved by the factor of 2. The evidence that this was associated with reversed shear came from the simulation. It takes into account the deep reduction in central temperature with the pellet injection and the strong bootstrap current density driven by the pressure gradient, which was found to be ballooning mode unstable with the usual monotonic q profile.

A regime of very high central $\beta(44\%)$ in DIII-D is found in 1992 [138]. It was achieved by a ramped shaping technique, which led to reversal shear, again as measured by the equilibrium reconstruction and location of the rational surface via MHD signals. The core region had also such high pressure gradients that this could only be explained in terms of the access to second stability afforded by reversed shear.

Research into reversed shear plasmas has recently been revolutionized by two new developments; the motional Stark effect (MSE) diagnostic which provides a local measurement of the direction of B, and new current-ramp techniques for producing reversal shear reliably and controllably, if transiently. Numerous tokamak such as JET, Tokamak Fusion Test Reactor (TFTR), DIII-D and Japan Torus-60 Upgrade (JT-60U) are now studying the reversed shear mode with these techniques.

A.4.3 Monotonic q profile case

The Glad-Shafranov equation in a cylindrical coordinate system (r, z, ϕ) is,

$$-\Delta^*\Psi = -\left(r\frac{\partial}{\partial r}\frac{1}{r}\frac{\partial}{\partial r} + \frac{\partial^2}{\partial z^2}\right) = r^2\mu P' + TT', \tag{A.1}$$

where Ψ is a stream function. It is defined as $\Psi = \Psi_{pol}/2\pi$, where Ψ_{pol} is a poloidal flux. To solve this equation, pressure function P and toroidal function T should be given. We use a gauss type function defined as,

$$\frac{dP}{d\Psi} = c\,b_p\{\exp(1-x^\lambda)-1\}, \qquad T\frac{dT}{d\Psi} = c(1-b_p)\,R_0^2\{\exp(1-x^\lambda)-1\}, \tag{A.2}$$

where $x = (\Psi - \Psi_0)/(\Psi_s - \Psi_0)$, suffix 0 and s denote the value at the plasma axis and on the plasma surface. The three parameter, (c, b_p, λ), characterize the plasma equilibrium. c define the value of plasma current, therefore, we optimize the rest two parameters to find the critical beta.

EQLAUS/ERATO codes can check the MHD instability such as Mercier criterion, Ballooning instability, and kink instability. The wall surrounding the plasma is located the infinity, and we check the $n = 1$ kink instability, where n is the toroidal number. The results is shown in Fig. A.7. The critical beta is 2.57 (normalized beta, also known as Toroyon coefficient, $\beta_N = 2.64$). The plasma equilibrium, the current profile, the pressure profile and others are show in Fig. A.8. The q profile is monotonical increase.

Next, we use DRIVER code to realize the current and the pressure profile determined above calculations by the non-inductive current drive, such as NBCD. Figure A.9 shows the results. NBI of 1.0 MeV and 60 MW is enough to produce the objective profile. We can denote the difference of the center of q profile, however, it is come from the flaw of the code. The bootstrap current ratio is 54 % and the neutron wall loading is 1.1 MW/m^2 as listed in Table. A.2.

A.4.4 Reversed shear profile case

More freedom degree for the equilibrium is needed for making the reversed shear q profile than previous monotonic q profile case to find the critical β. We used 8 parameter type function for P and T defined as,

$$\frac{dP}{d\Psi} = c\,p_2(1-x^{p_3})\{p_4+(1-p_4)x^{p_5}\}, \qquad T\frac{dT}{d\Psi} = c\,R_0^2(1-x^{t_2})\{t_3+(1-t_3)x^{t_4}\} - R_0^2P'. \tag{A.3}$$

The result which beta is critical for MHD instability by EQLAUS/ERATO codes is shown in Fig. A.10. The wall surrounding the plasma is located as $b/a = 1.3$. The plasma is stable to the kink modes with $n = 1, 2, 3$. This result is consist with Ref. [139], modeling the DIII-D's reversed shear plasma. The critical beta is 3.04 ($\beta_N = 3.13$) in this calculation.

The necessary non-inductive current drive power is calculated by DRIVER code and the result is shown in Fig. A.11. The NBI of 55 MW, 1.0 MeV is enough to produce the objective profile, but mainly the non-inductive current flow the surrounding region. When LHRF could use for its current, NBI decrease to 10 MW, 1.0 MeV and LHRF of 15 MW which is supported the periphery current. If NBI energy is decreasing from 1.0 MeV to 0.55 MeV, then the demand NBI power is 24.5 MW as shown in Fig. A.12. The bootstrap current ratio is 77 % and the neutron wall loading is 1.3 MW/m^2 listed in Table. A.2. These value are larger than that of standard q profile.

A.5 Summary

Volumetric neutron source (VNS) has been designed by 0D system design code, and it has confirmed that the maximum of neutron wall loading is higher than 1MW/m^2.

From the view point of plasma equilibrium, the pancake winding is better than the layer winding for the center solenoid coil of VNS. The demand power of poloidal field system is about 200 MW.

The maximum β values were derived by MHD stability analysis with ERATO code, 2.8% for the monotonic q profile and 3.8% for the reversed shear profile. The appropriate auxiliary heating power which is the neutral beam injection (NBI) with 60 MW was derived by DRIVER code for realizing the proper current distribution of the monotonic q profile. In the case of the reversed shear profile, the 20% higher neutron flux wall was derived than the monotonic q profile one. The power of NBI for the reversed shear profile would be reduced from 55.0MW (beam energy is 1.0MeV) to 24.5MW (0.55MeV) if the lower hybrid resonant frequency heating (LHRF) with 14.7MW were used.

Table A.1: Major parameter of ITER EDA, IDLT, and VNS.

	ITER (EDA)	IDLT	VNS
plasma major radius R [m]	8.14	10.0	4.5
plasma minor radius a [m]	2.80	1.87	1.0
aspect ration A	2.91	5.35	4.5
elongation κ	1.6	1.85	1.8
triangulation δ	0.25	0.4	0.24
plasma volume $V_{\rm p}$ [m^3]	2016	1277	160
plasma current $I_{\rm p}$ [MA]	21	13.9	5.6
plasma temperature T [keV]	10.5	15	12
plasma density n [10^{20}m^{-3}]	1.3	1.24	1.2
maximum toroidal filed $B_{\rm t}$ [T]	12.5	12	12.5
auxiliary power $P_{\rm aux}$ [MW]	100	40	70
fusion output $P_{\rm f}$ [MW]	1500	2700	270
pulse length	1000sec.	$\sim$10hrs.	steady-state

Table A.2: Parameter list of VNS. q profile of standard and advance are the monotonic profile and the reversed shear profile, respectively.

parameter	standard	advance	
heating method	NBI	NBI	NBI + LHRF
wall loading P_W [MW/m^2]	1.1	1.3	1.3
plasma major radius R[m]	4.5	4.5	4.5
aspect ratio A	4.5	4.5	4.5
elongation κ	1.8	1.8	1.8
triangulation δ	0.24	0.24	0.24
average electron temperature $\overline{T_e}$[keV]	11.9	11.2	11.3
average ion temperature $\overline{T_i}$[keV]	13.7	11.7	11.4
average electron density $\overline{n_e}$[m^{-3}]	0.97×10^{20}	1.37×10^{20}	1.17×10^{20}
helium concentration f_{He}	5%	5%	5%
effective charge number Z_{eff} (He, C, O, Fe)	1.5	1.5	1.5
plasma current I_p	5.67	5.45	5.40
bootstrap current ratio I_{bc}/I_p	54%	77%	77%
toroidal field B_t [T]	5.83	5.83	5.83
safety factor q_Ψ	3.04	3.10*	3.10**
H-mode factor f_H	2.1	2.6	3.0
toroidal beta β_t [%]	2.8	3.5	3.5
normalized beta β_N	2.8	3.8	3.8
neutral beam energy E_b [MeV]	1.0	1.0	0.55
neutral beam power P_B [MW]	60.1	55.0	24.5
LHRF power P_{rf} [MW]	0	0	14.7
fusion output P_f [MW]	307	386	381
energy gain Q value	4.7	6.4	9.7

* $q_{min} = 2.15, q_0 = 2.61$, ** $q_{min} = 2.17, q_0 = 2.61$

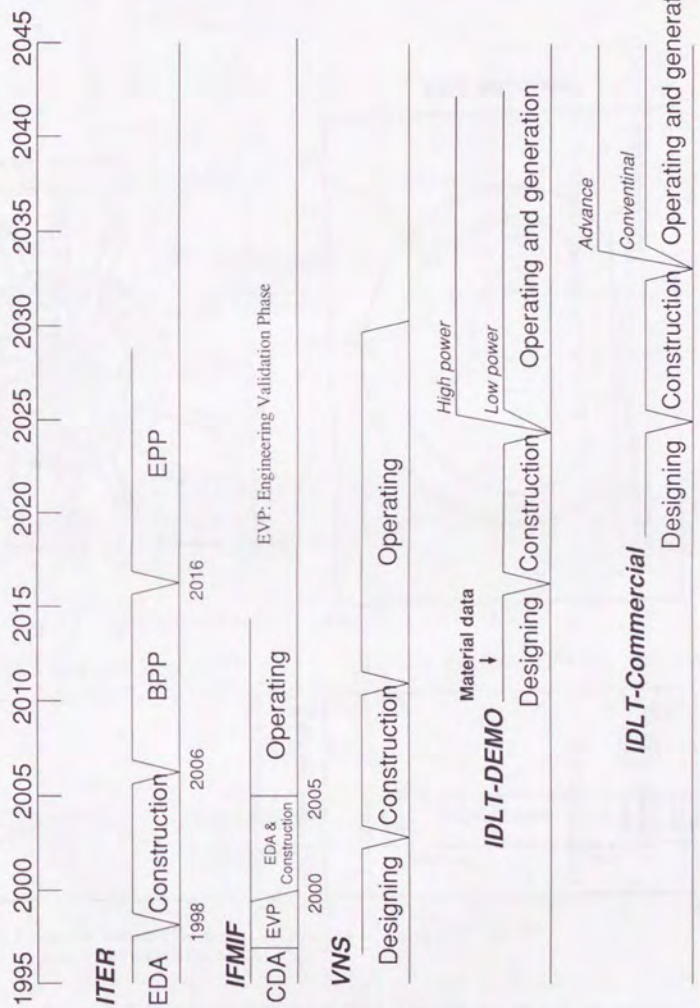

Figure A.1: Time schedule of ITER, VNS, and IDLT series.

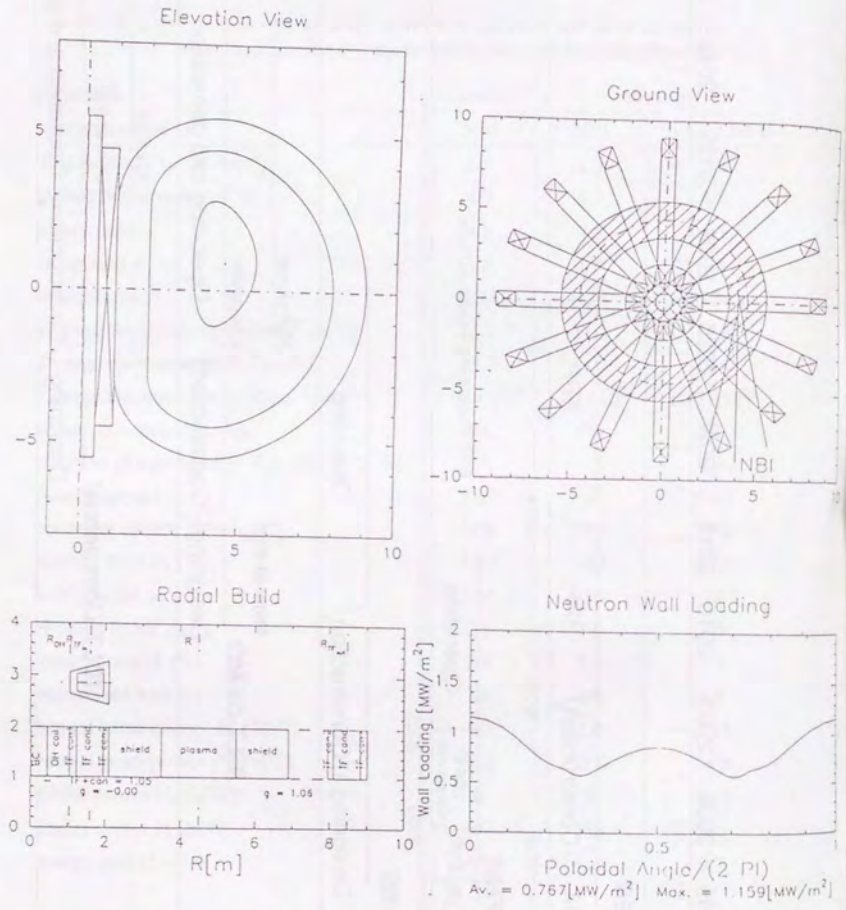

Figure A.2: Results of 0D system code for VNS.

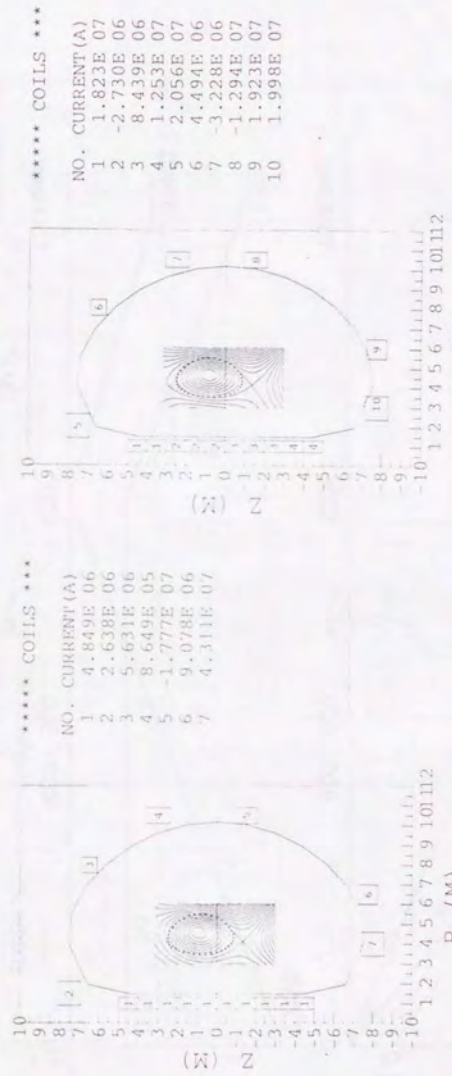

Figure A.3: Plasma equilibrium of VNS. The stored energy of the pancake winding is much smaller than that of the layer winding.

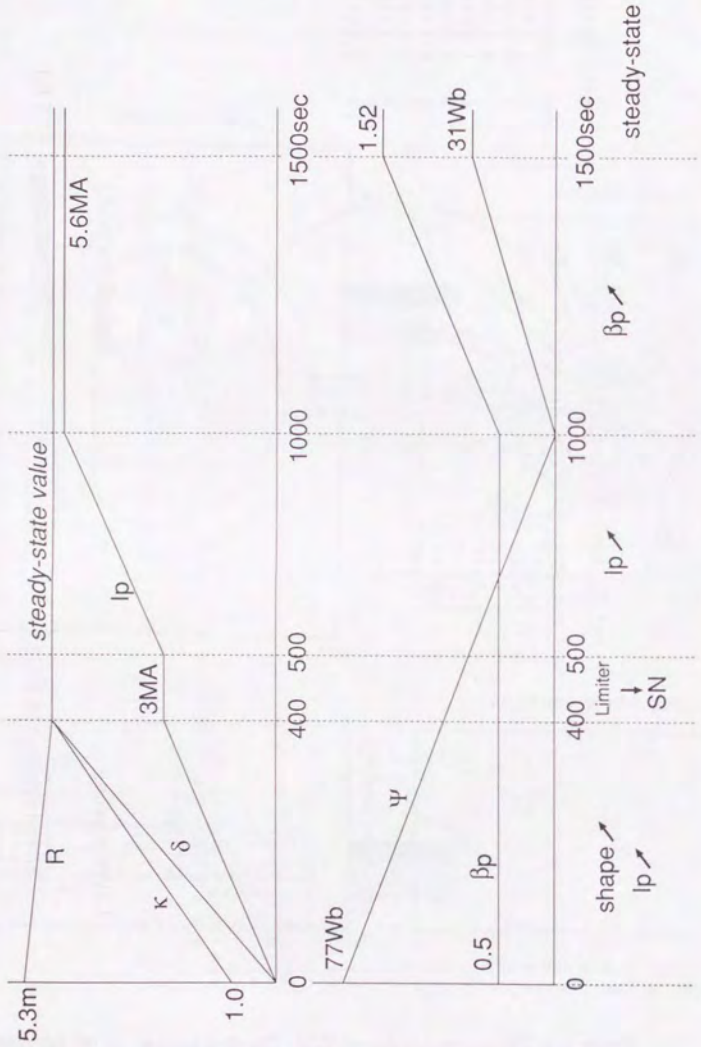

Figure A.4: Parameter variation in the ramp-up phase.

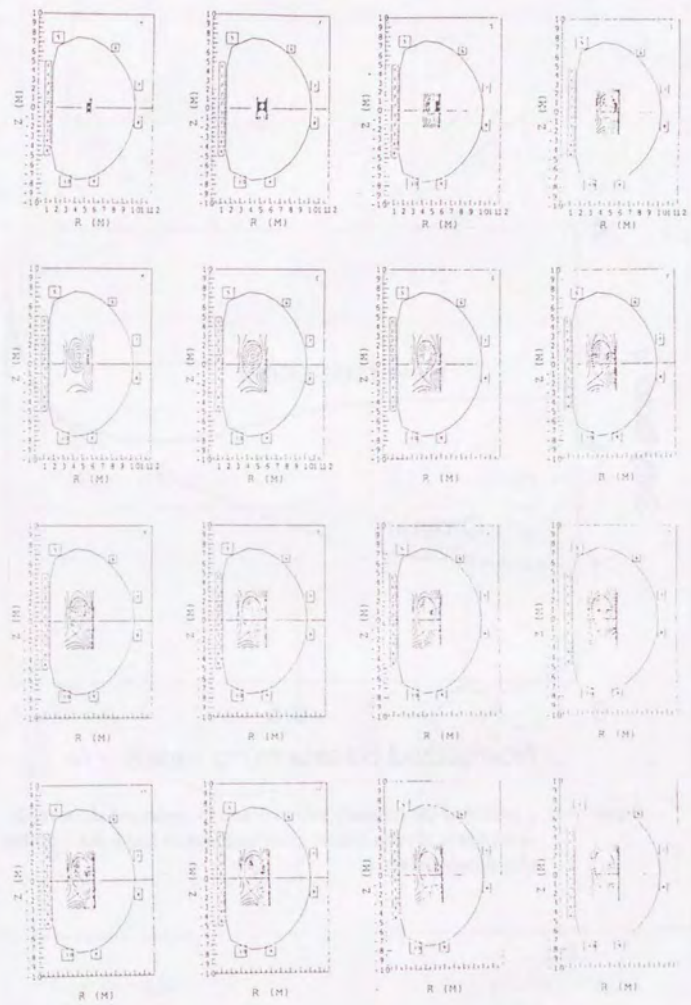

Figure A.5: Plasma equilibrium of VNS in the ramp-up phase. The order is from the upper-left to the lower-right.

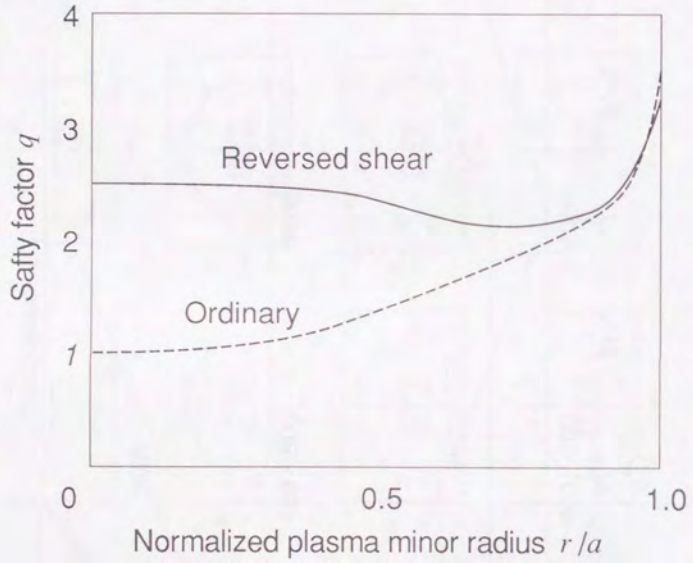

Figure A.6: q profile of the ordinary tokamak and the reversed shear mode. Solid line is reversed shear mode and broken line is the q profile of ordinary tokamak.

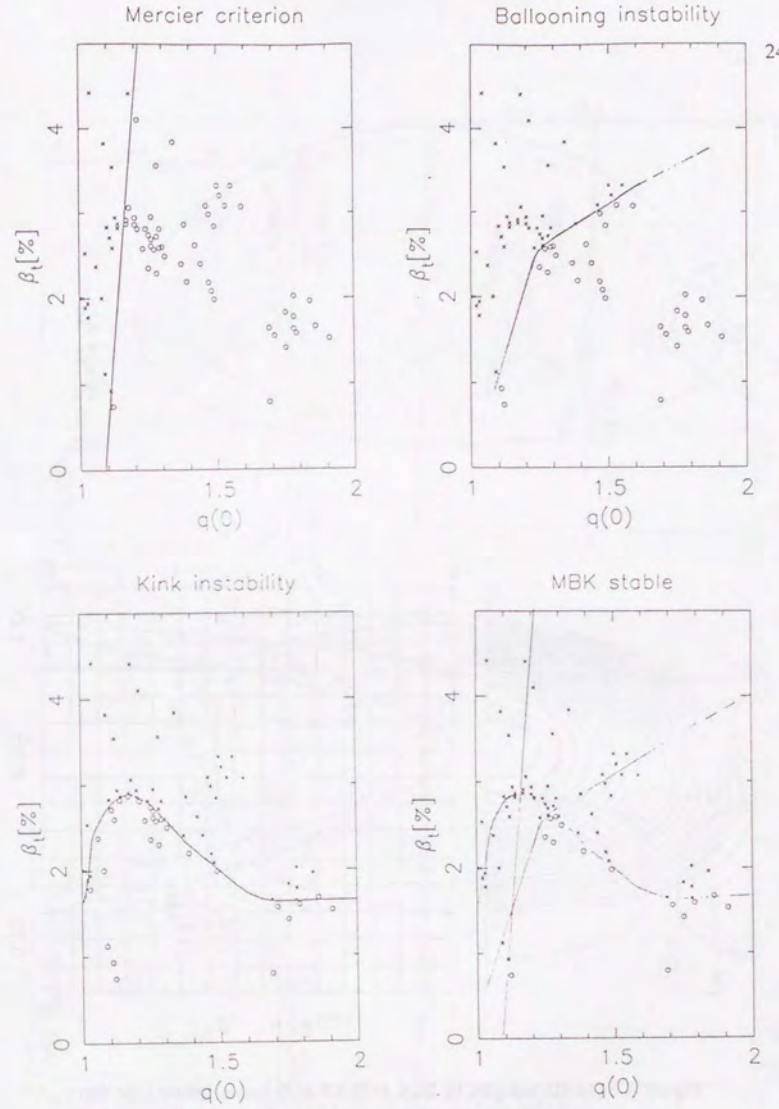

Figure A.7: MHD instability analysis by EQLAUS/ERATO codes (gauss type function). The circle and cross denote the stable and the instable at the position.

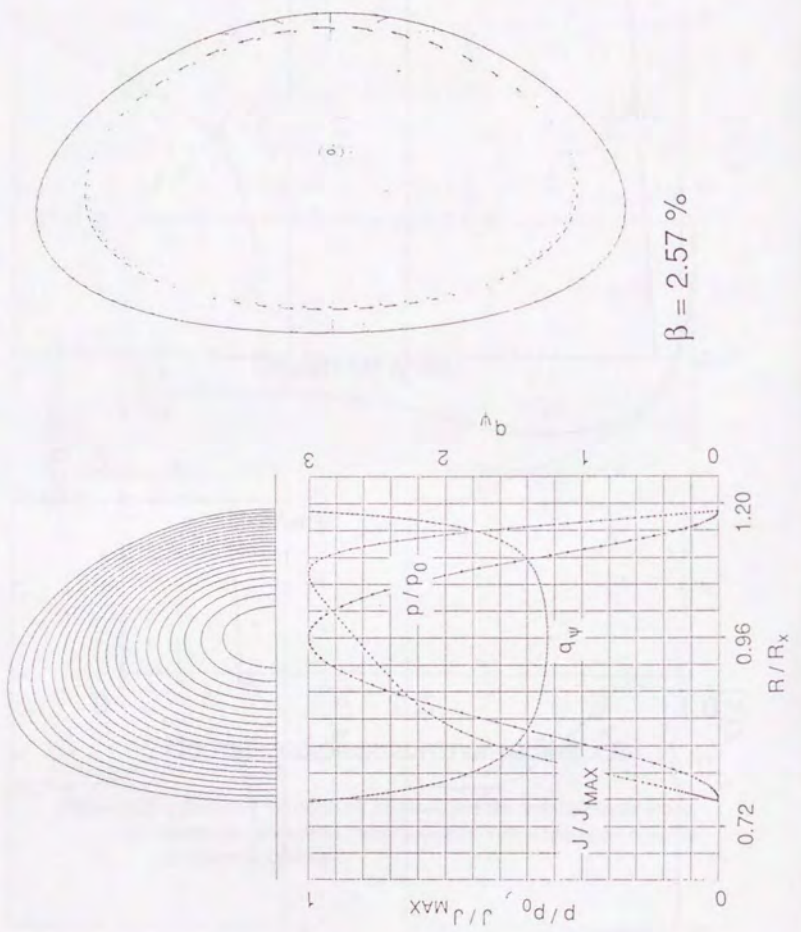

Figure A.8: MHD analysis by EQLAUS/ERATO codes (gauss type function). Plasma equilibrium surface is denoted at the upper-left. The current, the pressure and q profile is denoted at lower-left. The maximum eigen-vector of the kink mode(n = 1) is shown on the right.

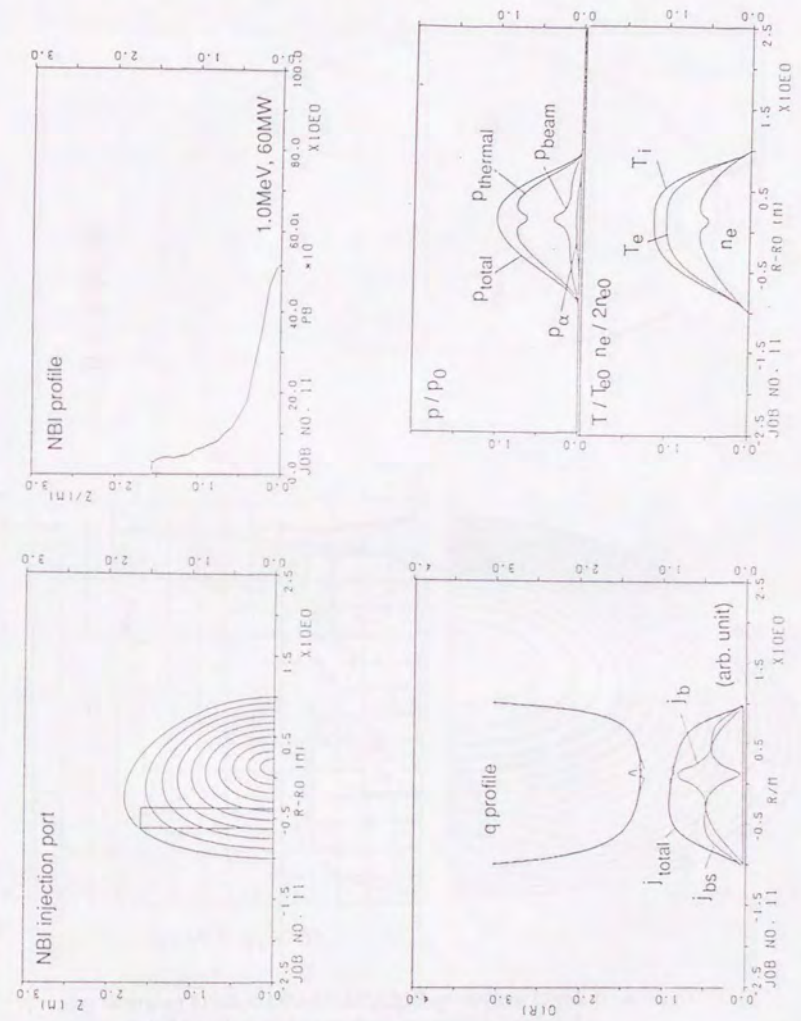

Figure A.9: Various parameter profile by DRIVE code (gauss type function). The necessary NBI is 60MW (1.0MeV).

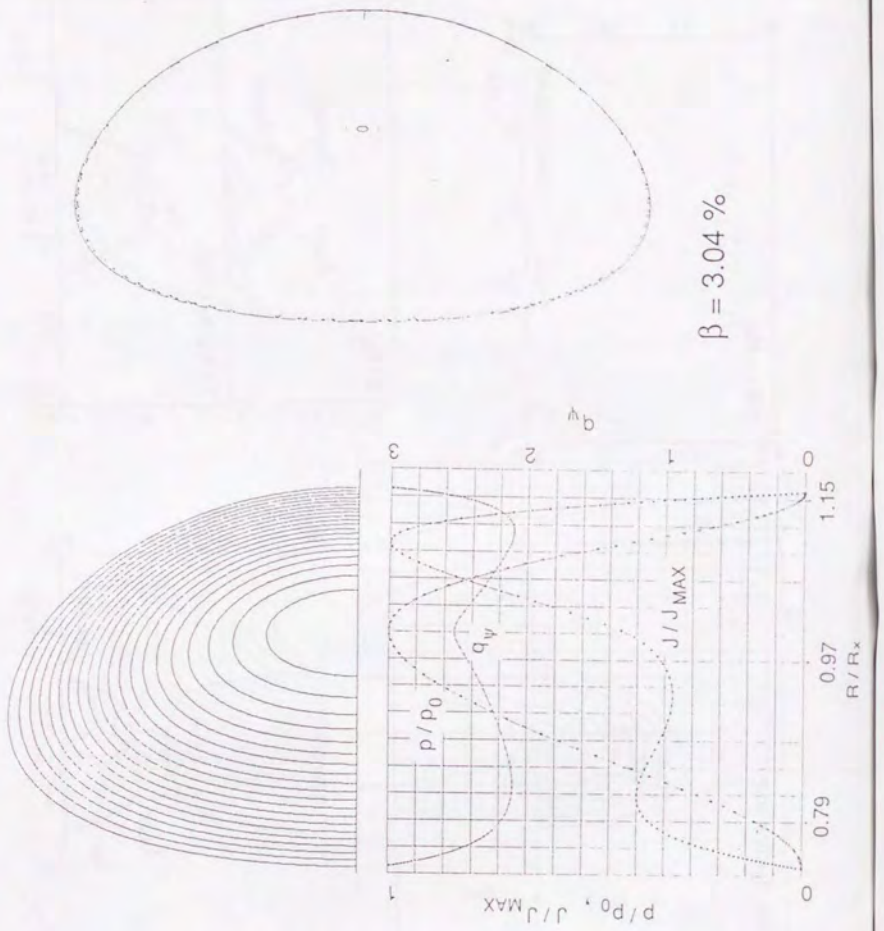

Figure A.10: MHD analysis by EQLAUS/ERATO codes (8 parameter type function). Plasma equilibrium surface is denoted at the upper-left. The current, the pressure and q profile is denoted at lower-left. The maximum eigen-vector of the kink mode(n = 1) is shown on the right.

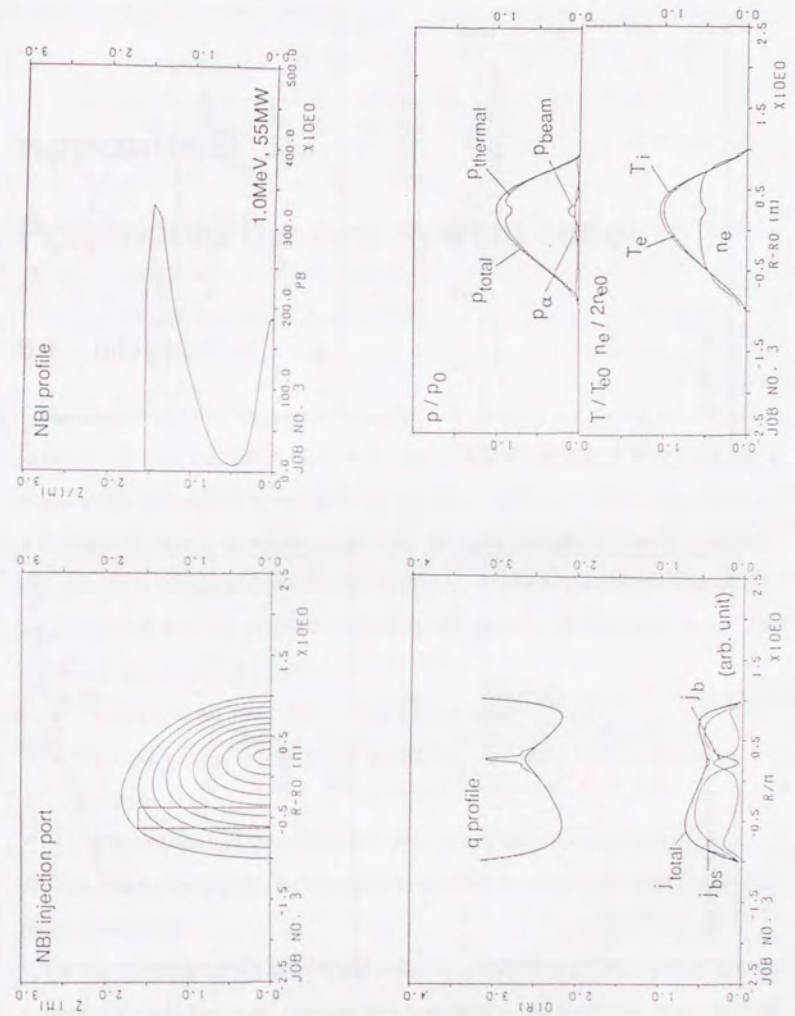

Figure A.11: Various parameter profile by DRIVE code (8 parameter type function; NBI). The necessary NBI is 55MW (1.0MeV).

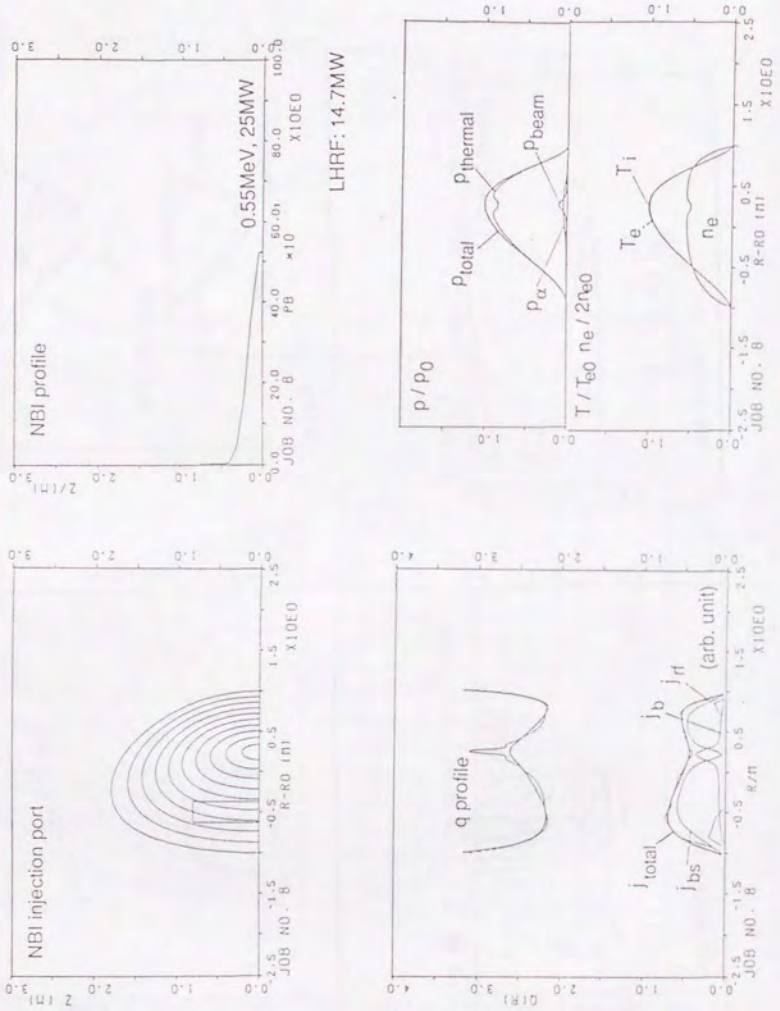

Figure A.12: The various parameter profile by DRIVE code (8 parameter type function; NBI+LHRF). The necessary NBI is 25MW (0.55MeV) with the LHRF of 15MW.

Appendix B

Proposal of the new system code

B.1 Introduction

The physical and the engineering parameters are surveyed for finding the optimized parameter set when the fusion reactor is designed. The fusion reactor is simulated as a simple model or a sophisticate model for the parameter survey. The calculation, however, is complicated on even the simple model case. We use a specialized code for each field, such as, Plasma OPeration CONtor (POPCON) plot, ramp-up of the plasma, plasma equilibrium, plasma transport, magnetic field of the coil, neutron shielding, and so on. The demerits of this style are following:

- The format of the data input and output is not unify.
- The input and the output data is handled by the manual between the codes, not automatic.
- The optimization of the parameter between the codes is not easy work.

To reduce such a complexity, the some system code are developed and widely used in the fusion community.

The high-dimensional precision model make the system code so large that it is difficult to modify and add the model from the new knowledge. The restriction comes primary from the programming language. To overcome the limitation we propose the system code for the tokamak fusion reactor by the object-oriented language. The main feature is that

the modules are loosely coupled each other, the latest physical and engineering model could flexibly combine with the system code. We will use it for Inductively Driven Long pulsed Tokamak (IDLT) rector, Volumetric Neutron Source (VNS), and so on.

The next section, section 2, the concept of the object-oriented technology and the object-oriented language, C++, are described. We will first develop the 0 dimensional (point-model) system code for the prototype, and then the physical and engineering module is development or use the existing code as the module. These modules are first exist on one machine, then the module are distributed the machines connected the network. These are explained in Section 3. The conclusion is in Section 4.

B.2 Object-oriented technology

The most existing software are written by the procedural programming language, such as COBOL, Fortran, and C language. The software is getting larger, the problems of the extendibility and the maintainability are often occurred. Therefore, an object-oriented language which has the inheritance, the information hiding, and the polymorphism is now paying the attention.

B.2.1 Object orient-oriented technology

What is the object-orient technology?

The object consist of a set of data and its operation. The object-oriented programming is made that to pass the message to the object. The object has a following feature.

inheritance The object can get a character of the other object. The object is hierarchal classified by the inheritance.

encapsulate The information of the object is hided (information hiding), and cannot access the information from the outer-world. The information can contact only by the interface from the outer-world.

polymorphism The object acts the characteristic works when the same message was passed to the relative objects.

The usual software engineering is stressed one of the process, the data, the several type of the state, and the event. These four elements can be handled by the object-oriented technology.

In the C and the other procedural programming languages, programming tends to be action-oriented, whereas in C++ language tends to be object-oriented. C++ is the one of the object-oriented programming. In C, the unit of programming is the function. In C++, the unit of programming is the *class* from which objects are eventually instantiated (*i.e.* created) [140].

C programmers concentrate on writing functions. Groups of actions that perform some common task are formed into functions, and functions are grouped to from programs. Data is certainly important in C, but the view is that data exists primary in support of the actions that functions perform. The verbs in a system specification help the C programmer determine the set of functions that will work together to implement the system.

C++ programmer concentrate on creating their own user-defined types called *classes*. Each class contains data as well as the set of functions that manipulate the date. The data components of a class are called data members. The function components of a class are called member functions. Just as an instance of a built-in type such a `int` is called a variable, an instance of a user-defined type (*i.e.* a class) is called an *object*. The focus of attention in C++ is on objects rather than functions. The nouns in a system specification help the C++ programmer determine the set of classes from which objects will be created that will work together to implement the system.

The feature of object-orient technology

The merits

- The detail of the process can be hided. It help the programmer to read the code.
- The data and its operations can be encapsulated. The improvement of the code and re-use is rather easy.
- The code can be divided between the interface and the implementation. This can be help the group work.

The demerits

- The concept of object-oriented technique is complex, it take the time and cost for learning it.
- The runtime speed is not faster than the code made by the procedural programming.
- The merit of object-oriented technique is exaggerated. "***No silver bullet.***" [141].

The example of the object-orient program in the fusion field

One of the example of the the object-orient program in the fusion field is gyro-kinetic simulation on Numerical Tokamak Project (NTP) [142–144] . The explanation of NTP is described the following paragraph [145].

Numerical Tokamak Project A tremendous amount of development remain before fusion can be applied to the commercially successful generation of electricity. Future experiments will be large and expensive, costing as much as several billions of dollars each. Such machines must be designed to perform optimally allowing the little room for uncertainty. High-performance computing is playing a profoundly important role in analyzing the equilibrium, the stability, and the transport of all current major fusion experiments.

The most elusive problem of tokamak design and operation is the anomalous loss of plasma particles and energy. The experiments observe turbulent fluctuations driven by collective modes of the oscillation and losses that always exceed the rates calculated for a quiescent plasma. Such collective fluctuations enhance the transport of heat in a plasma in

much the same way that fluid turbulence in ocean waves or eddies in the atmosphere enhance heat transport rates. An understanding of these processes and of their scaling with parameters as the parameters evolve is so critical to tokamak development that in 1988 the Department of Energy (DOE) began a focused the study of transport. While impressive progress has been made, a key difficulty is the detailed calculation of the solution to plasma turbulence equation. Recent increases in the power of massively parallel computers, when combined with both advances in theory, which have simplified these equations, and improved numerical method have now made feasible a direct numerical simulation of the plasma turbulence. The Numerical Tokamak Project (NTP) is a U.S. effort to carry out this work. It comprises a consortium of researches at six national laboratories of the DOE and the National Aeronautics and Space Administration (NASA), five universities, the National Energy Research Supercomputer Center at Livermore, the Advanced Computing Laboratory at Los Alamos, and the High Performance Computer Center at Oak Ridge.

Numerical studies of the plasma confinement in a tokamak are complicated by several factors. Perhaps the most important is the extreme range of time scales in a fusion plasma, extending from 10^{-12} s for the fast electrons to several seconds, the time scale required for the plasma profile to relax to a true steady state. The fluctuations of greatest interest have time scales in the range of a fraction to several milliseconds.

Great efforts have been made during the past decade to develop model equations and appropriate algorithms that embody theses complex processes. Both the fluid and the particle approaches have been extended in the direction of each other. For example, particle-in-cell (PIC) methods, initially developed to examine the fastest time scales in a collision less plasmas, have been extended into the low-frequency regime of interest by gyroaveraging, numerical orbit averaging, and implicit techniques. On the other hand, fluid approaches originally applied to describe large-scale magnetohydrodynamics phenomena have been

modified to include the essential kinetic affects associated with the nearly free motion of a plasma particle along the magnetic field.

The NTP is adapting both approaches to provide alternative numerical treatments in a region where the times scales overlap (Figure B.1). If validated in the overlap region, fluid models, which require many fewer degrees of freedom that PIC models, may provide a much mode efficient means of studying the transport. Comparisons of the fluid and PIC approaches are quantifying approximations in the former and several issues related to the numerical precision of the latter, including how the shot noise of individual particles affects the numerical solutions. Figure B.2 presents a schematic of advances in both modeling and more powerful computers that are contributing to the NTP.

The NTP plans for the future research include expanded use of existing and new massively parallel computers to perform additional simulations studying the scaling of tokamak turbulence with respect to the important physical parameters and more comprehensive simulations with physics models augmented to include additional physics. Of particle interest is the inclusion of kinetic electron, electromagnetic, and trapped-particle effects. The success of the NTP in developing advanced parallel algorithms and new implicit and perturbative methods is providing the foundation to support the addition of new physics and ensure that the more comprehensive models will make the best use of the available computing resources.

B.2.2 Object-oriented language

C++

The C++ language [146,147] is a general-purpose programming language that is, except for miner details, a superset of C. It improves on C [148] through its support of data abstraction and object-oriented programming [149]. The main influences on its design, in addition to C, were Simula67 and Algol68 (Figure. B.3).

C++ was first installed 1983. Today, it has several independent implementations and many thousands of installations. It is being used for major university research project and for large-scale software development in companies. It has been applied to most branches of programming, including banking, CAD, compiler construction, networking, scientific computation, and very-large-scale-integration design.

C++ is distinguished among languages that support object-oriented programming, such as Smalltalk, by a variety of factors; its emphasis on program structure; the flexibility of encapsulation mechanisms; its smooth support of a range of programming paradigms; the portability of C++ implementations; the run time efficiency in both time and space of C++ code; and its ability to run without a large run-time system.

C++ has a single, very flexible, type system. This makes it possible to use hybrid programming styles without violating the C++ type system. It also lets you choose a style of programming closely matching individual application areas.

Fortran90

Fortran is far from being the only programming language available on most computers. In the course of time new languages have been developed, and where they were demonstrably more suitable for a particular type of application they have been adopted in preference to Fortran for that purpose [150]. Fortran's superiority has always been in the area of numerical, scientific, engineering, and technical applications, and there is still no significant competitor in these fields. The Fortran community has a truly vast investment in Fortran codes, with many programs (some of 100,000 lines or more) in frequent use. This does not mean, however, that the community is necessarily completely content with the language, and in order that it be brought properly up-to-date, the ANSI-accredited technical community X3J3 has once again prepared a new standard, formally known as Fortran 8x and now as Fortran 90.

As well as standardizing vender extensions, there is a need to modernize it in response to the developments in language design which have been exploited in other languages, such ad APL, Algol 68, Pascal, and Ada. Here, X3J3 can draw on the obvious benefits of concepts like data hiding. In the same vein is the need to begin to provide an alternative to dangerous storage association, to abolish the rigidity of the outmoded source form, and to improve future on the regularity of the language, as well as to form, and to improve further on the regularity of the language, as well as to increase the safety of programming in the language and to tighten the conformance requirements. To preserve the vast investment in Fortran 77 codes, the whole of Fortran 77 is contained as a subset.

However unlike the previous standard, which resulted almost entirely from an effort to standardize exiting practices, the new standard is much more a development of the language, introducing features which are new to Fortran, but are based on experience in other languages. The most significant new feature are the ability to handle arrays using a concise but powerful notation, and the ability to define and manipulate user-defined data types. The first of these will lead to a simplification in the coding of many mathematical problems, and will also make Fortran a more efficient language on the new generation of supercomputers as these array features are well matched to their hardware. The second enables programmers to express their problems in terms of data types exactly matched to their requirements.

The new feature contained in Fortran 90 should ensure that the Fortran language will continue to be used successfully for a long time to come. The fact that it contains the whole of Fortran 77 as a subset means that conversion to Fortran 90 will be as simple as conversion to another Fortran 77 processor.

B.2.3 Method of software development

The software development could be described generally the following list:

- Analysis
- Design
- Implement
- Test

"Analysis phase" is that take an information from the problem or the event. In object-oriented programming, this phase is the most important. The real world is convert to the model. "Design phase" is the constant the model to refine the relation between the modules. Using the design map, the model is covered to the programming language at "Implement phase". In object-oriented programming, this phase is not so important. It require only the technique for convert the the relation as the modules to the programming language. At last, after the converting to the code is finished, "Test phase" is that check the code is right for the problem of the event. These test are very important for the program. If the code does not satisfy the requirement, we must return the "Design phase" or "Analysis phase".

There are many method for the analysis and design the problem for object-oriented programming. Object Modeling Technique (OMT) method is one of them [151]. The software development could be described as the following list by OMT method.

1. Object Analysis

   Problem description The requirement is described in the document. The aim of this phase is that make the object clear.

   Construct of the object model The objects and classes are recognized from the document made in the problem description. Next, find the relation between the objects and classes and add the attribution to the object and the class. The chart of the object model is used in this latter phase.

   Construct of the active model The active model describes the relation of the system or objects on the time. The event trace diagram is used for this phase.

Construct of the functional model The functional model is describes only how to the value calculate and ignore the calculation order, criterion decision, and the object structure. The functional model describes the mathematical function. The data flow diagram is used in this phase.

2. Object Design

System design The system design consists the determination of the set of the sub-system for the system, the allocation of the sub-system from the hardware and the software elements, and the decision of a primary concept and a policy from the detail system design.

Object design In the object design phase, the classes and its relations are completely defined, and the interface for the method and the algorithm are also defined.

3. Implement

Figure B.4 – B.8 is shown the dependence of each module in the case of tokamak reactor. These diagrams are the class diagrams by OMT method. In this figure, two important concept is there, aggregation and generalization. An aggregation is a relation of "has – a", for example, "Tokamak has a coil system". An generalization is a relation of "is – a", for example, "Center solenoid coil is a (kind of) poloidal coil". The model for the tokamak fusion reactor is built through this analysis. The model is a baseline for coding the system code for tokamak reactor.

Figure B.9 shows the event trace diagram of the system code for the tokamak reactor. The time flows from the top to the bottom in this figure.

B.3 Implementation

B.3.1 Objects of the system code

The primary objects of a new system code are listed below.

- Take account of the extendibility of the modules to add or modify the model.
- Simple, easy understandable operation.
- More time, more precision results (rank up the dimension of the model).
- Store the calculation results and the input data. They can be referred if they are needed.
- The program language which is used in the system code is C++ (the partly, Fortran is used).

In the background of above object, the workstation and the personal computer is rapidly higher performance and the lower cost.

B.3.2 Network distributed code

Figure B.10 is the existing system code. All module is running on the single machine. Figure. B.11 is the network distributed type system code. The codes are distributed on the machines connected with network. The grain of parallel computing is very large. The module (grain) on the machine is a independence each other, we call this state "loose coupled" computing. The merit of this method is that the existing code could be incorporate with a few changes. The network protocol is TCP/IP. The hetero-machines can be used in this method because the difference between the machine architecture assimilate with interface part. The RPC protocol would be used for this purpose.

B.4 Conclusion

The abstract of object-orient technology is described and the software development is investigated. The tokamak fusion reactor is modeled and the mutual relation is shown by

the OMT method.

The new object-oriented system code has been proposed. This code is worked on the workstation and/or personal computer. The modules are distributed on the computers on the network. The modules are loosely coupled, therefore, the existing code could be fitted easily.

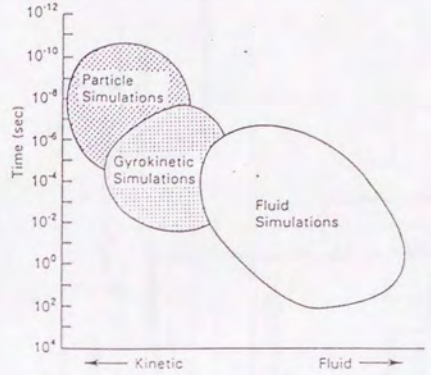

Figure B.1: Schematic of time scales and regions of applicability for fluid and kinetic simulation models in magnetic fusion [145].

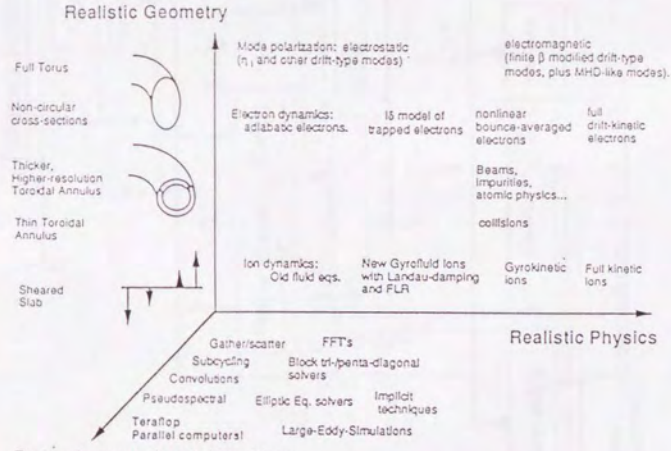

Figure B.2: Schematic of computational advances in modeling tokamak turbulence [145].

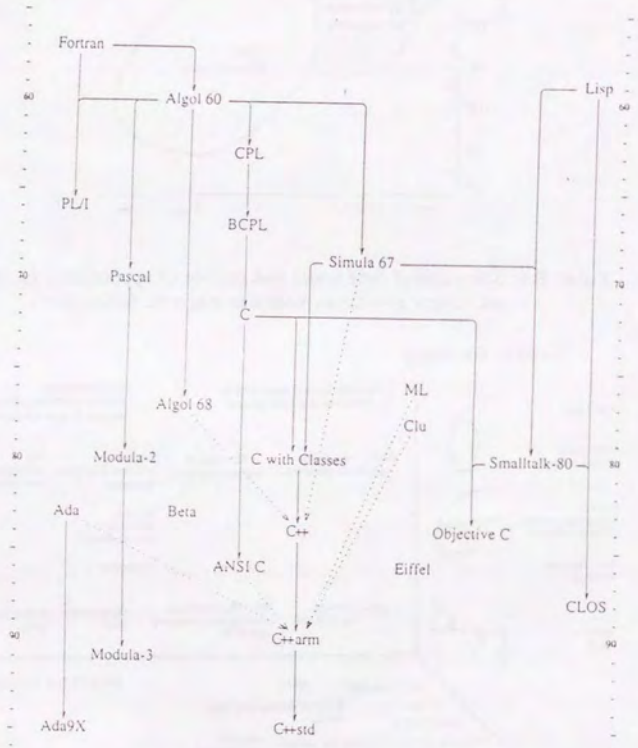

Figure B.3: History of the programming language [152].

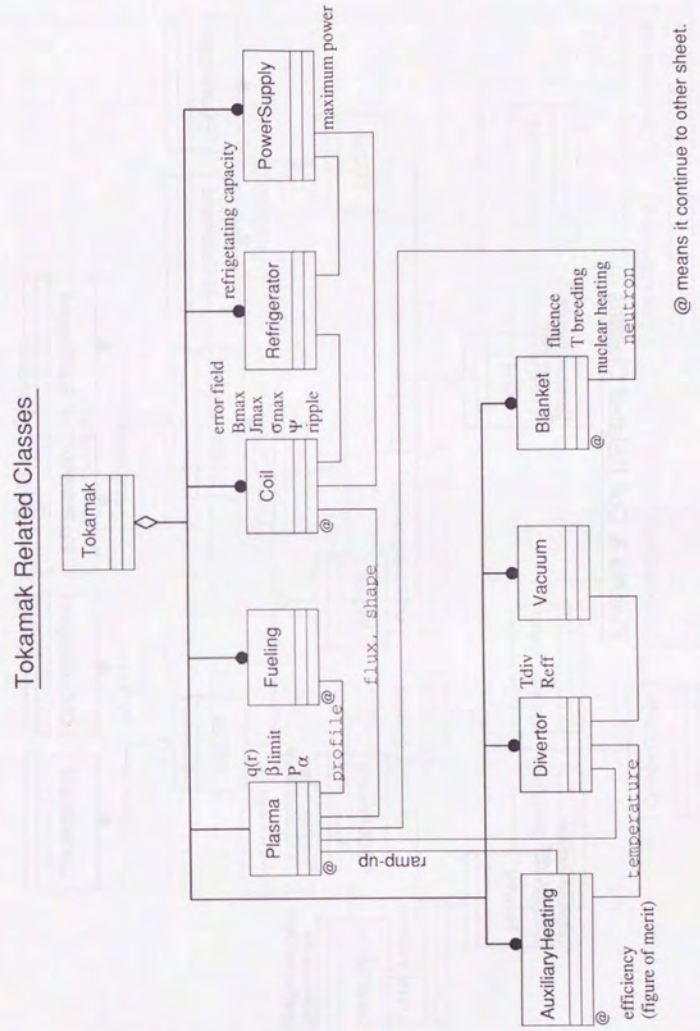

Figure B.4: Tokamak related classes. The legend is shown in Fig. B.8.

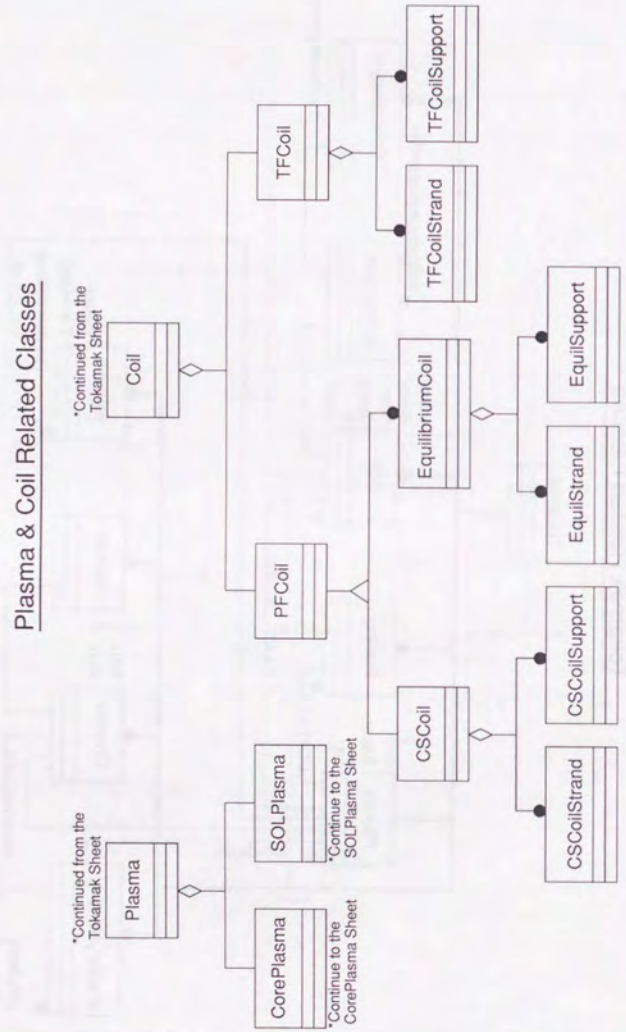

Figure B.5: Plasma and coil related classes. The legend is shown in Fig. B.8.

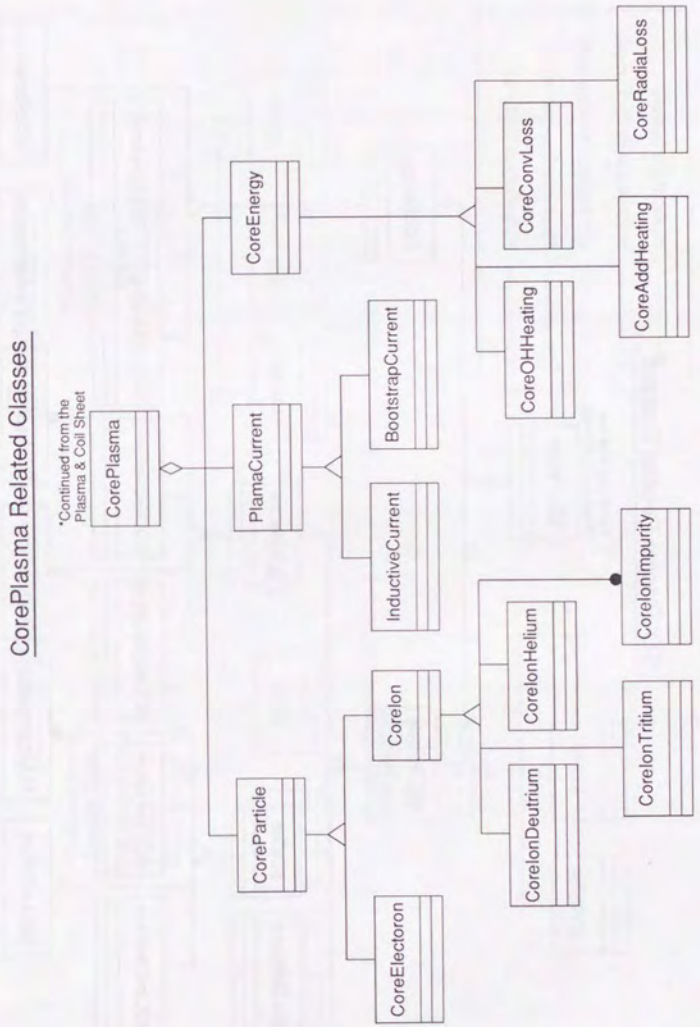

Figure B.6: Core plasma related classes. The legend is shown in Fig. B.8.

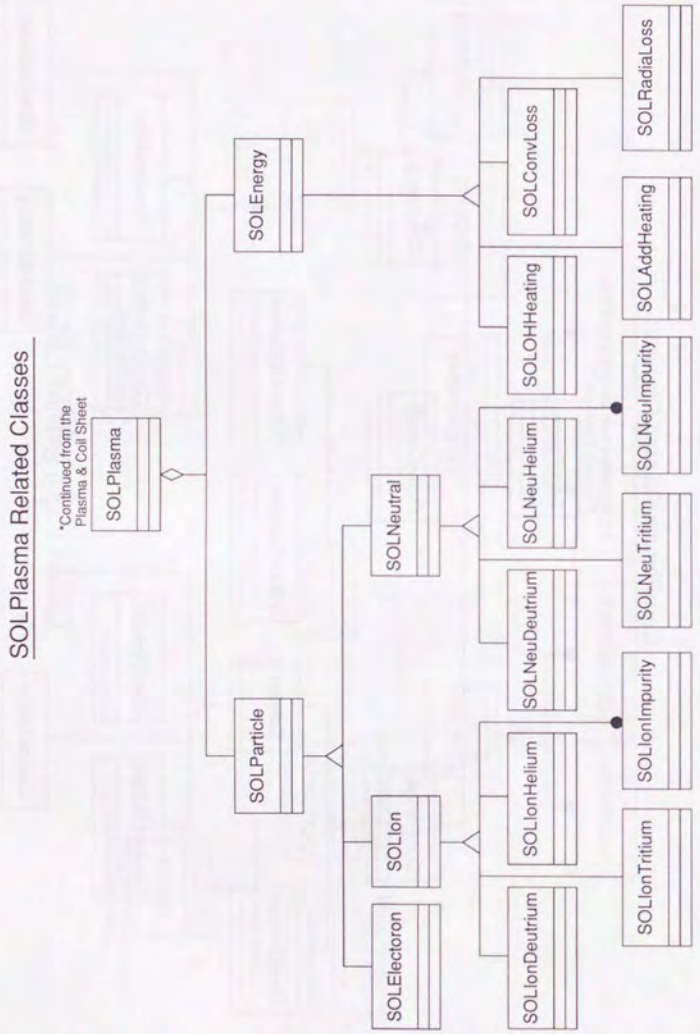

Figure B.7: SOL plasma related classes. The legend is shown in Fig. B.8.

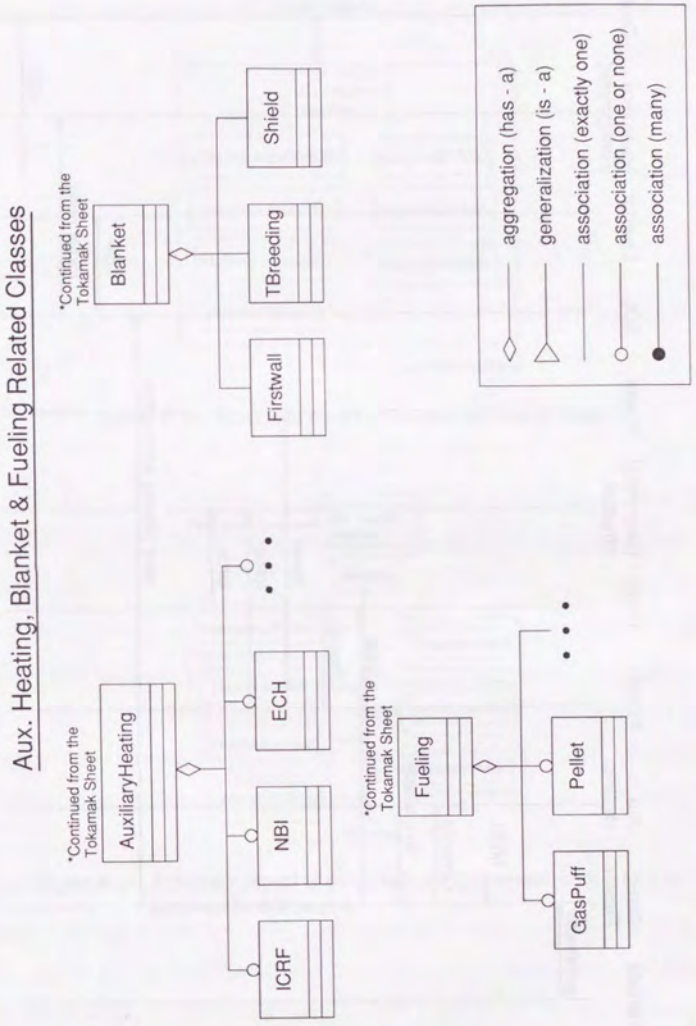

Figure B.8: Auxiliary heating, blanket and fueling system related classes.

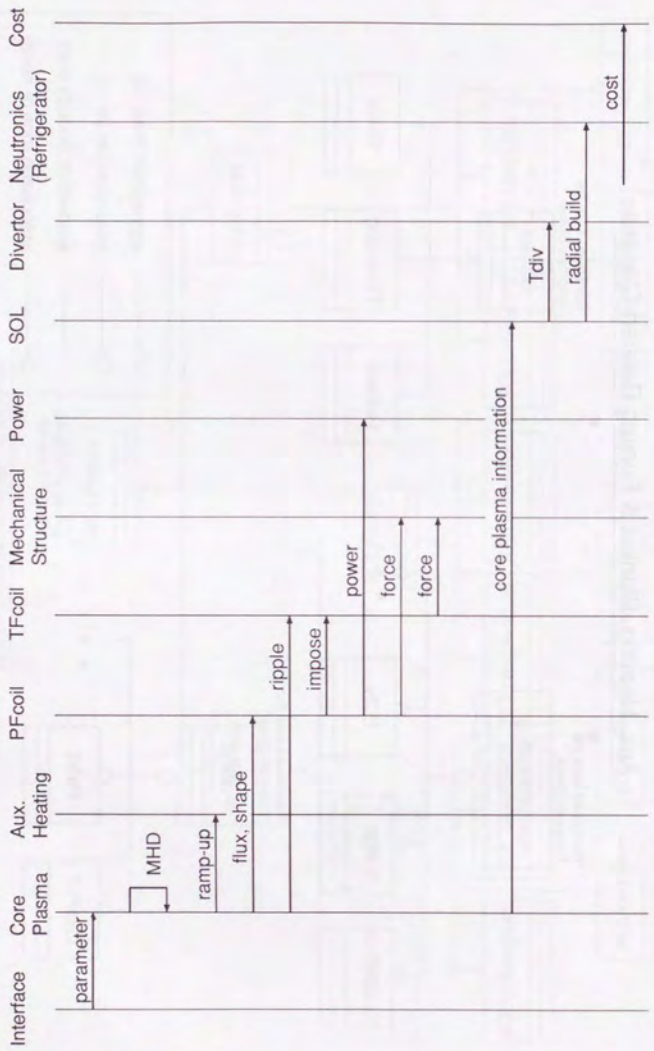

Figure B.9: Event trace diagram of the system code for the fusion reactor.

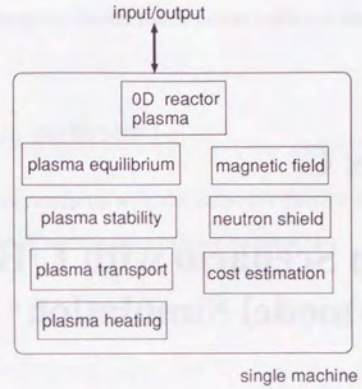

Figure B.10: Schematic model of the existing system code.

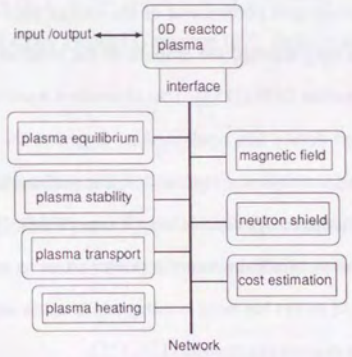

Figure B.11: Schematic model of the distributed-type system code which is proposed in this section.

Appendix C

Ramp-up Scenario with L/H Transition by Point-model Simulation

C.1 Introduction

H-mode, the improvement phenomena of the energy confinement, was discovered by ASDEX team when they injected the amount of the external power to the main plasma by neutral-beam injection (NBI) [153]. This H-mode is a universal phenomenon, because many fusion-oriented device has confirmed it. It makes the commercial reactor design more realistic. In the recent fusion reactor designs, such as ITER [55], IDLT [54], SSTR [64] and ARIES-I [9], the energy confinement is expected the H-mode. It is experimentally clear that there exists a minimum heating power so as to access H-mode confinement region. This threshold power has been investigated in many tokamak devices, and recently compiled with some plasma parameters [154, 155].

In this section, we simulate the plasma ramp-up of International Thermonuclear Experimental Reactor, Engineering Design Activity (ITER EDA) by using the 0 dimensional (0D) simulation based on a power balance equation and a helium (He) particle balance equation with L- to H- and H- to L-mode transitions. We also compare the results with plasma operating contour plot (POPCON plot) [84]. We adopt the new ramp-up method, where the surface area of the plasma is varied during ramp-up for saving the auxiliary

heating power for the ignition. Simple fusion power control is also examined in this section.

C.2 Simulation methods

We simulate the plasma ramp-up with the 0D power balance equation and the helium particle balance equation. The 0D power balance equation is

$$\frac{dW_{\rm p}}{dt} = P_\alpha + P_{\rm OH} + P_{\rm aux} - P_{\rm Brad} - P_{\rm sync} - P_{\rm cond} \ , \tag{C.1}$$

where $W_{\rm p}$[MJ] is plasma thermal energy, and P_α, $P_{\rm OH}$, $P_{\rm aux}$, $P_{\rm Brad}$ and $P_{\rm sync}$ are the total powers of alpha particle heating, Ohmic heating, additional heating, Bremsstrahlung loss and synchronous radiation loss, in MW. The confinement loss $P_{\rm cond}$ is defined as $P_{\rm cond} = W_{\rm p}/\tau_{\rm E}$, where $\tau_{\rm E}$[s] is the global energy confinement time. Details of these terms are given in ITER CDA Physics Guideline [49]. Helium particle balance equation is

$$\frac{dn_\alpha}{dt} = -\frac{n_\alpha}{\tau_{\rm p}^*} + \frac{P_\alpha}{E_\alpha}(+S_\alpha) \ , \tag{C.2}$$

where $n_\alpha[10^{20}/{\rm m}^3]$ is the helium particle density, E_α is the the releases energy at a deuterium-tritium fusion reaction (3.5MeV) and $S_\alpha[10^{20}/{\rm m}^3]$ is the external injected the helium particles for suppressing the excess of the fusion power. The parameter $\tau_{\rm p}^*$[s] is the effective particle confinement time defined as

$$\tau_{\rm p}^* = \frac{\tau_{\rm p}}{1 - R_{\rm eff}} \ , \tag{C.3}$$

where $\tau_{\rm p}$[s] is the particle confinement time and $R_{\rm eff}$ is the effective recycling ratio [156]. We approximate that $\tau_{\rm p}^* \simeq 10\tau_{\rm E}$ and adjust the ratio of $\tau_{\rm p}^*$ to $\tau_{\rm E}$ to the required fusion power.

Many scaling laws for the energy confinement time are proposed. Here we use the combination of Neo-Alcator law and ITER 89 L-mode power law. The energy confinement

time τ_E is taken as follows [50],

$$\frac{1}{\tau_E} = \left(\frac{1}{\tau_{NA}^2} + \frac{1}{\tau_{EH}^2} \right)^{1/2} , \tag{C.4}$$

where τ_{NA}[s] is Neo-Alcator OH confinement time [51], and τ_{EH} is the energy confinement time for the auxiliary heated plasmas. The Neo-Alcator confinement time takes the form,

$$\tau_{NA} = 0.07 n_{20} a R^2 q_* , \tag{C.5}$$

where $\langle n_{20} \rangle$ [10^{20}/m^3] is the volume-averaged electron density, R[m] and a[m] are the plasma major and minor radii and q_* is the cylindrical equivalent safety factor expressed by

$$q_* = \frac{5 a^2 B_0}{R I_p} \frac{1 + \kappa^2 (1 + \delta^2 - 1.2\delta^3)}{2} , \tag{C.6}$$

where B_0 [T] is the toroidal field at the plasma center, The parameter I_p[MA] is the total plasma current, κ is the elongation of the plasma and δ is the triangularity of the plasma. For the energy confinement time of auxiliary heated plasmas, the enhanced ITER-89 power law scaling [49] is adopted which is given by

$$\tau_{EH} \equiv f_H \times \tau_E^{ITER89P} , \tag{C.7}$$

$$\tau_E^{ITER89P} = 0.048 A_i^{0.5} I_p^{0.85} R^{1.2} a^{0.3} \kappa^{0.5} \bar{n}_{20}^{0.1} B^{0.2} P_{in}^{-0.5} , \tag{C.8}$$

where f_H is the H-factor, the enhancement factor from the L-mode, A_i is the ionic mass number, and P_{in}[MW] is total heating power defined by

$$P_{in} = P_\alpha + P_{OH} + P_{aux} - P_{Brad} - P_{sync} . \tag{C.9}$$

We choose f_H of 1.0 as L-mode and f_H of 2.0 as H-mode. The criterion for distinguishing between L- and H-mode is depended on the threshold power P_{th},

$$P_{th} = 0.04 n_{20} B_t S , \tag{C.10}$$

where S[m^2] is the plasma surface area [154]. The H-factor has a hysteresis effect; The L/H transition takes place when P_{in} is larger than P_{th}, and the H/L transition dose when P_{in} is smaller than 50% of P_{th} as shown in Fig. C.1.

With these equations, we simulated the plasma ramp-up with ITER EDA parameters [58]. The cross section of the plasma at the flattop is shown in Fig. C.2 and the main parameters is listed in Table C.1.

C.3 Results

C.3.1 POPCON plot and 0D simulation

To compare the results between POPCON plot and 0D simulation, we simply assume that the plasma is always H-mode and the plasma shape parameter(R, a, κ, and δ) and the helium particle fraction f_α is also constant during the ramp-up phase. Figure C.3 shows the POPCON plot on the ITER EDA parameter with the helium particle fraction of 0.11. Operating point is located on the line which is indicated the fusion power P_f of 1.5GW. Troyon coefficient of 3.0 is also shown in this figure.

The heating power P_{aux} of 20MW is sufficient for the ignition in this case because the heating power at the saddle point is about 17MW. The time-dependence 0D simulation confirms that the heating power of 20MW for 80 seconds is enough to ignition in this case as shown in Fig C.4.

It seems good agreement between POPCON plot and 0D simulation, if some transient parameters such as the helium fraction are assumed to be constant during the ramp-up phase. POPCON plot, however, could not take the following transient effects during the ramp-up phase into account:

1. The fraction of the impurity is not constant during the ramp-up phase as the steady state,
2. The H-mode can not be realized from the initial phase, but POPCON plot is assumed

that the plasma is always H-mode.

3. The cross section of the plasma is constant such as flattop.

Figure C.5 shows the POPCON plot with the initial impurity condition f_o = 0.03. The heating power $P_{\rm aux}$ at the saddle point is about 10MW, which is 60% of $P_{\rm aux}$ in Fig. C.3. The necessary heating power might be estimated to be smaller than that of previous POPCON plot. From the result of 0D simulation, the heating power of 12MW can also ignite the plasma, while the excess of the fusion power is occurred on the latter half of the ramp-up phase.

Mitarai overcomes one of the POPCON-plot's disadvantage, the plasma is always H-mode, by separating the $\langle T\rangle$-$\langle n\rangle$ space between the L-mode region and H-mode region, however, the impurity fraction is constant on his work [157].

C.3.2 Fixed-full-size ramp-up simulation

The 0D simulation with L/H transition determined by Eq. (C.10) are described here. The initial plasma state is assumed to be L-mode, and kept this state till $P_{\rm in} > P_{\rm th}$. Figure C.6 shows that the heating power of 70MW is needed for the ignition, which is about six times larger than that of the steady H-mode plasma. If we inject the heating power smaller than that of 70MW, H/L transition takes place the latter half of the ramp-up phase.

C.3.3 Reshaped-size ramp-up simulation

There are two methods for reducing the heating power; one is the start-up with the low density n_{20} and the other is the start-up with the small surface area S because $P_{\rm th} \propto n_{20}S$. The former method, the low density with the large external inject power, might cause the severe damage to the divertor plate. We propose the latter method, where the plasma is started with the small surface area and the relatively high density. On the ITER EDA plasma, the initial cross section of the plasma is the small circular, and the plasma is gradually grown up with the non-circular cross section, as shown in Fig. C.2 and listed in

Table. C.1. The heating power might be decreased to about half of 70MW when the ratio of plasma surface area between the initial phase and the flattop phase is take into account. We, however, restrict the plasma current $I_{\rm p}$ because of stabilization of magnetohydrodynamics(MHD) instability by $q_* \geq 3$, the heating power of 50MW is needed as shown in Fig. C.7.

On the other hand, if we inject the heating power of 70MW as same as previous case, we can start the plasma ramp-up with the initial density up to $0.45 \times 10^{20}/{\rm m}^3$. The divertor plate is mitigated compared with the constant cross section case. The excess of the fusion power also takes place. Many methods are proposed to suppress such a excess of the fusion power [91]. Here we adopt the impurity control method, the helium particle injection. To simplify the simulation, we assume that the helium particles injected to the plasma are rapidly diffused in the whole plasma and exhausted with the effective particle confinement time $\tau_{\rm p}^*$. We can control the fusion power within the 10% excess as shown in Fig. C.8, when the helium particles of 2.0×10^{20}/s are added in 25 seconds.

C.4 Conclusion

A new method for ramp-up scenario; *i.e.*, the start-up with the small plasma surface instead of the low plasma density, is proposed with the results of the simple 0D time-dependence simulation estimated L/H transition. The auxiliary power for ramp up can be decreased by new method compared with the usual scenario. The necessary auxiliary heating power is about 50MW with new method, while 70MW with full-size start-up scenario in the ITER EDA parameter. When the heating power of 70MW is injected into small-surface-area plasma, the initial plasma density can be increased from $0.30 \times 10^{20}/{\rm m}^3$ to $0.45 \times 10^{20}/{\rm m}^3$. Such high density operation might mitigate the erosion of the divertor plate.

The fusion power excess takes place in the latter half of the ramp-up phase. It is sup-

pressed within 10% by the external injection of the helium particles in the case of ITER EDA. The effect on the poloidal field coil system in this new start-up scenario is the future work.

Table C.1: Main plasma parameters of ITER EDA. The surface area of the plasma is varied for the decrease of the heating power.

parameter	flattop	ramp-up phase
major radius R [m]	8.1	fixed
minor radius a [m]	3.0	$2.0 \rightarrow 3.0$
elongation κ	1.55	$1.0 \rightarrow 1.55$
triangularity δ	0.20	$0.0 \rightarrow 0.20$
toroidal field B_t [T]	5.7	fixed

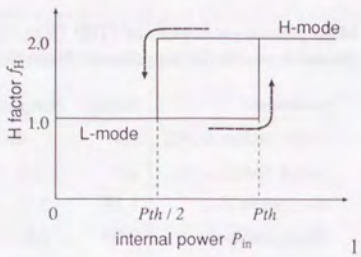

Figure C.1: H-factor f_{H} as a function of the threshold power P_{th}. The H-factor has a hysteresis effect.

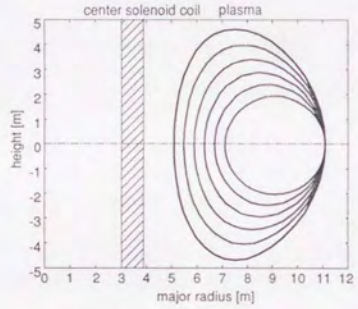

Figure C.2: Cross section of ITER EDA plasma during the ramp-up phase and at the flattop. The center solenoid coil is also shown in this figure. The plasma cross section is grown from the small circular to the non-circular during the ramp up phase.

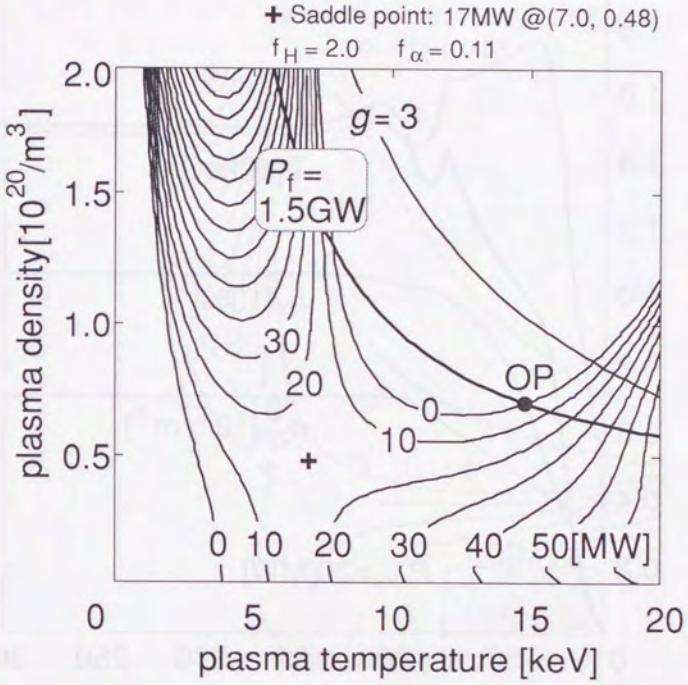

Figure C.3: POPCON plot for ITER EDA plasma. Beta limit with Troyon factor g of 3 and the fusion reactor output P_{f} of 2.7 GW are also shown. The saddle point is indicated by "+" symbol.

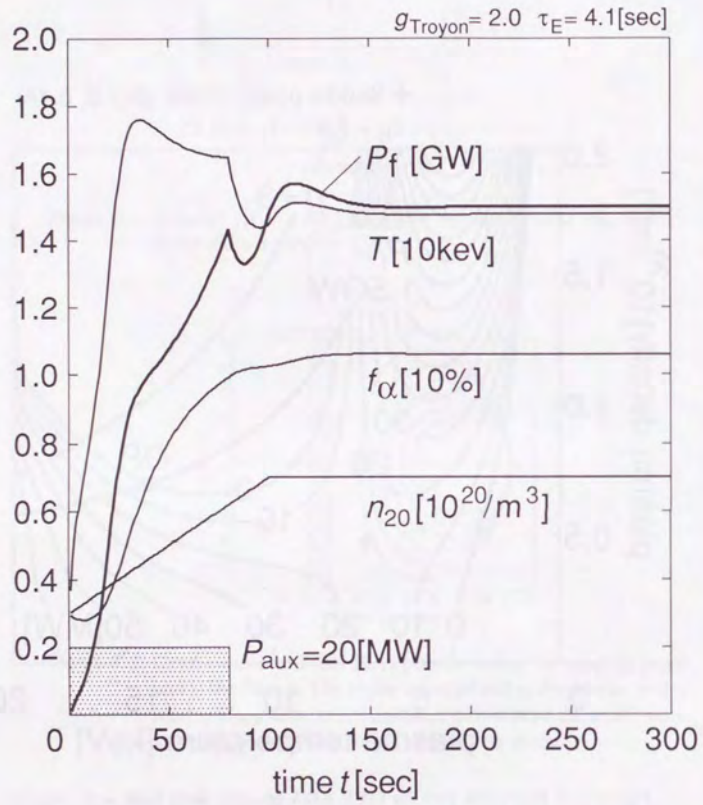

Figure C.4: Auxiliary heating power $P_{\rm aux}$ necessary for ignition. $P_{\rm f}$ is the fusion power of GW, where T is the plasma temperature of 10keV, f_α is the helium particle fraction of 10%, n_{20} is the plasma density of $10^{20}/{\rm m}^3$, and $P_{\rm aux}$ is the auxiliary heating power of 10MW.

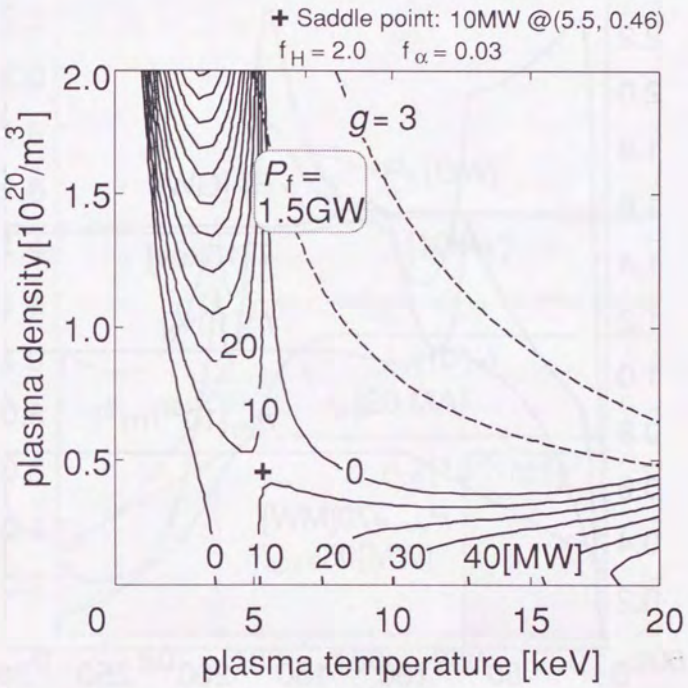

Figure C.5: POPCON plot for ITER EDA plasma at the initial phase, the helium particle fraction f_α is decreased to 0.03. The auxiliary power at the saddle point is reduced to 10MW.

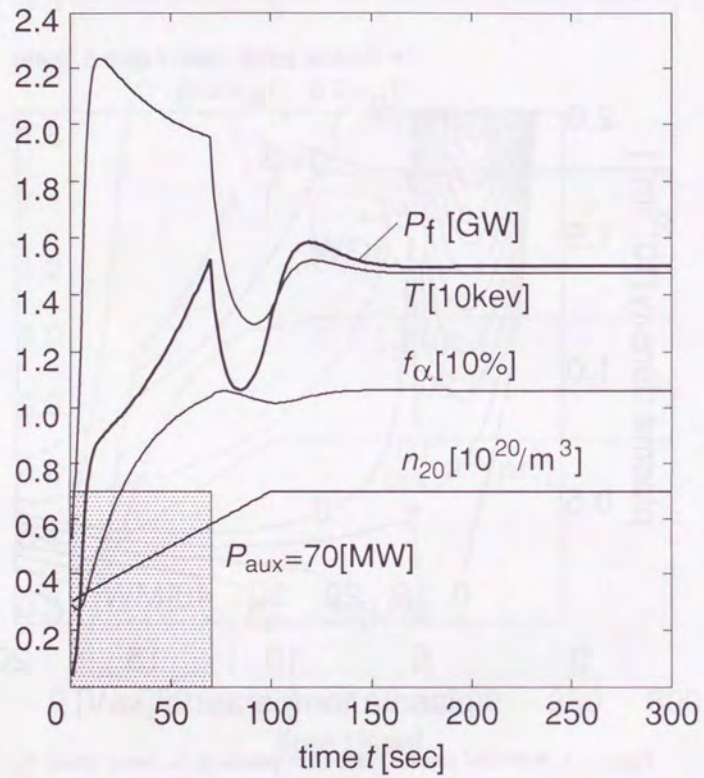

Figure C.6: Auxiliary heating power $P_{\rm aux}$ necessary for the ignition taken account of L/H and H/L transition. The heating power becomes about six times larger than that of the steady H-mode plasma.

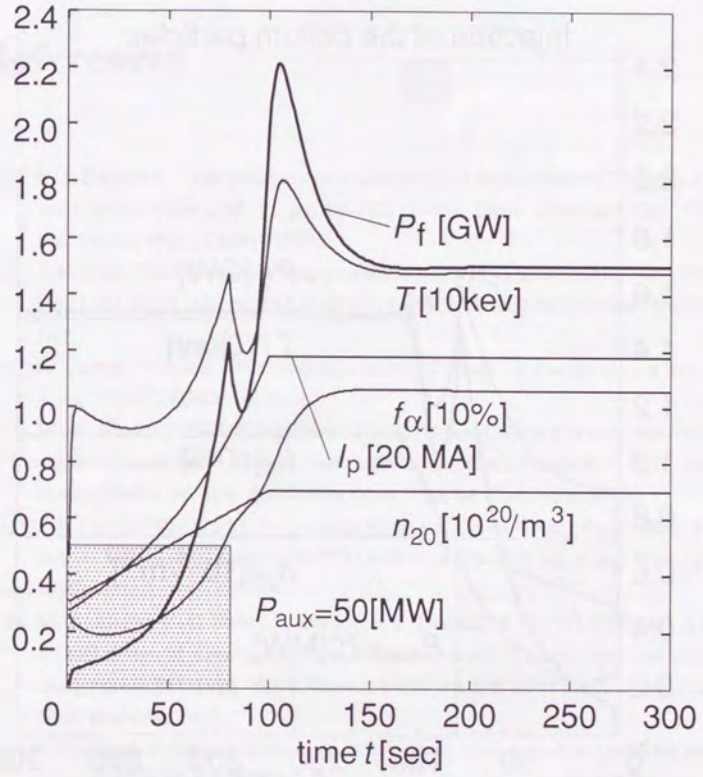

Figure C.7: Auxiliary heating power $P_{\rm aux}$ necessary for the ignition with the varying plasma surface area. The heating power is decrease to 50MW. The heating power is not so small because the plasma current $I_{\rm p}$ is restricted by the limitation; $q_* \geq 3$.

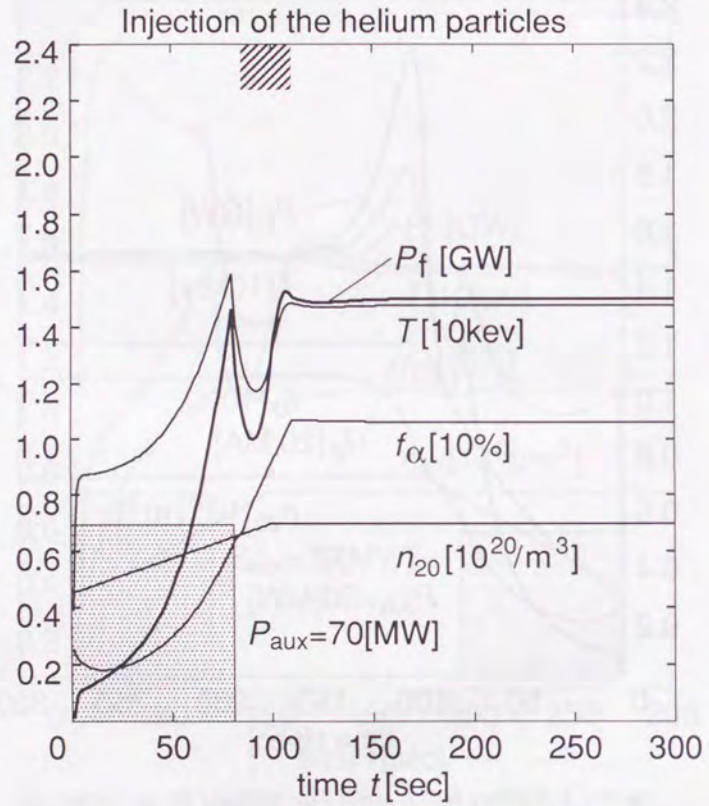

Figure C.8: Excess of the heating power P_f is suppressed by the helium particle injection. It is controlled within the 10% dispersion.

References

[1] R. J. Bickerton: "The purpose, status and future of fusion research", Plasma Phys. and Control. Fusion, **35**, 12, pp. B3–B21 (1993). (Proc. 20th Euro. Conf. Contr. Fus. Plasma Phys., Lisbon, 1993).

[2] P. K. Kaw: "Fusion power: Who need it?", Plasma Phys. and Control. Nucl. Fusion Res. 1993, Vol. 1, Vienna, IAEA, pp. 3–13 (1993). (Proc. 14th Int. Conf. Würzburg, 1992).

[3] K. Yamaji: "Nuclear fusion and environmental issues", J. Plasma Fusion Res., **69**, 4, pp. 305–312 (1993). (Salon).

[4] W. M. Stacey: "INTOR workshop: Design concept, critical issues, innovations, database assessment", Plasma Phys. and Control. Nucl. Fusion Res. 1988, Vol. 1, Vienna, IAEA, pp. 199–201 (1989). (Proc. 12th Int. Conf. Nice, 1988).

[5] J. F. Clarke: "ITER ad astra", Plasma Phys. and Control. Nucl. Fusion Res. 1991, Vol. 1, Vienna, IAEA, pp. 197–215 (1991). (Proc. 13th Int. Conf. Washington, 1990).

[6] M. A. Abdou, C. C. Baker, D. DeFreecs, C. Trachsel, et al.: "STARFIRE – A conceptual design of a commercial tokamak power plant", Plasma Phys. and Control. Nucl. Fusion Res. 1981, Vol. 2, Vienna, IAEA, pp. 119–131 (1981). (Proc. 8th Int. Conf. Brussels, 1980).

[7] M. Kikuchi, Y. Seki, A. Oikawa, T. Ando, et al.: "Conceptual design of the steady state tokamak reactor (SSTR)", Fusion Engrg. Des., **18**, pp. 195–202 (1991).

[8] M. Kikuchi and M. Azumi: "Experimental evidence for the bootstrap current in a tokamak", Plasma Phys. and Control. Fusion, **37**, pp. 1215–1238 (1995).

[9] R. W. Conn and F. Najmabadi: "ARIES-I, a steady-state, first-stability tokamak reactor with enhanced safety and environmental features", Plasma Phys. and Control. Nucl. Fusion Res. 1991, Vol. 1, Vienna, IAEA, pp. 659–672 (1991). (Proc. 13th Int. Conf. Washington, 1990).

[10] M. kikuchi, R. W. Conn, F. Najmabadi and Y. Seki: "Recent directions in plasma

physics and its impact on tokamak magnetic fusion design", Fusion Engrg. Des., **16**, pp. 253–270 (1991).

[11] E. J. Strait: "Stability of high beta tokamak plasmas", Phys. Plasmas, **1**, 5, pp. 1415–1431 (1994).

[12] F. Najimabadi, R. W. Conn and the ARIES TEAM: "Directions for attractive tokamak reactors: the ARIES-II and ARIES-IV second-stability designs", Plasma Phys. and Control. Nucl. Fusion Res. 1993, Vol. 3, Vienna, IAEA, pp. 295–310 (1993). (Proc. 14th Int. Conf. Würzburg, 1992).

[13] H. Y. Khater and the ARIES Team: "Activation analysis of the PULSAR-I fusion power reactor", 16th Symposium on Fusion Engineering (SOFE-16) (Eds. by G. H. Miley and C. Elliott)IEEE, IEEE, pp. 990–993 (1995).

[14] H. Y. Khater and the ARIES Team: "Activation analysis of the PULSAR-II fusion power reactor", 16th Symposium on Fusion Engineering (SOFE-16) (Eds. by G. H. Miley and C. Elliott)IEEE, IEEE, pp. 994–997 (1995).

[15] F. Najmabadi and the ARIES team: "Assessment of tokamak plasma operation modes as fusion power plants: the starlite study", IAEA (1996). (in 16th IAEA Fusion Energy Conference) IAEA-F1-CN-64/G1.

[16] C. G. Bathke and the ARIES team: "A system assessment of the five starlite tokamak power plants", ARIES Team Papers Presented at the ANS 12th Topical Meeting on the Technology of Fusion Energy: Collection of PreprintsUCSD, pp. 9–13 (1996). (UCSD-ENG-030, Fusion Technol. **25**(1996) ***to be published.***).

[17] S. Nishio, S. Ueda, I. Aoki, R. Kitamura, et al.: "Maintenance oriented tokamak reactor with low activation material and high aspect ratio configuration", IAEA (1996). (in 16th IAEA Fusion Energy Conference) IAEA-CN-64/GP-27.

[18] R. L. Reid, R. J. Barrett, T. G. Brown, G. E. Gorker, et al.: "The tokamak system code", Technical Report ORNL/FEDC-84/9, ORNL, Tennessee (1985).

[19] K. Borrass and M. Söll: "SUPERCOIL: A model for the computational design of tokamaks", Nucl. Engrg. Des./Fusion, **4**, pp. 21–35 (1986).

[20] S. Nishio, T. Tone, M. Kasai and M. Nishikawa: "Development of tokamak reactor systems analysis code "TORSAC"", Technical Report JAERI-M 87-021, JAERI (1987). (in Japanese).

[21] I. Group: "International Tokamak Reactor, Phase Two, Part I", IAEA, Vienna (1983).

[22] K. Sako, T. Tone, Y. Seki, H. Iida, et al.: "Design study of swimming pool type tokamak reactor SPTR", J. Nucl. Sci. and Technol., **19**, 6, pp. 491–503 (1982).

[23] T. Tone, M. Nishikawa and Y. Tanaka: "Design studies of tokamak power reactor in JAERI", Fusion Technol., **8**, 1, Part 2(A), pp. 731–740 (1985).

[24] T. Mizoguchi, M. Sugihara, K. Shinya, T. Kobayashi and othes: "Development of tokamak reactor conceptual design code "TRESCODE" –Conseptual design study of FY96 FER–", Technical Report JAERI-M 87-120, JAERI (1987).

[25] F. Najmabadi, R. W. Conn, et al.: "The ARIES-I tokamak reactor study", Technical Report UCLA-PPG-1323, UCLA (1991).

[26] K. A. Werley: "Reversed field pinch ignition requirements", Nucl. Fusion, **31**, 3, pp. 567–582 (1991).

[27] C. G. Bathke and the ARIES Team: "A preliminary system assessment of the Starlite demo candidate", 16th Symposium on Fusion Engineering (SOFE-16) (Eds. by G. H. Miley and C. Elliott)IEEE, IEEE, pp. 1139–1144 (1995).

[28] Y. Ogawa and N. Inoue: "Cost analysis of IDLT reactors using the ARIES system code", J. Plasma Fusion Res., **72**, 9, pp. 953–959 (1996).

[29] S. W. Haney, W. L. Barr, J. A. Crotinger, L. J. Perkins, C. J. Solomon, E. A. Chaniotakis, J. P. Freidberg, J. Wei, J. D. Galambos and J. Mandrekas: "A "SUPERCODE" for systems analysis of tokamak experiments and reactor", Fusion Technol., **21**, pp. 1749–1758 (1992).

[30] S. W. Haney and J. A. Crotinger: "C++ proves useful in writing a tokamak systems code", Comput. Phys., **6**, 5, pp. 450–455 (1992).

[31] S. W. Haney, J. P. Freidberg and C. J. Solomon: "A fast, user-friendly code for calculating magnetohydrodynamic equilibria.", Comput. Phys., **9**, 2, pp. 216–224 (1995).

[32] J. D. Galambos and L. J. Perkins: "Subignited, ITER-like designs – A question of confinement margin", Fusion Technol., **25**, pp. 176–181 (1994).

[33] J. D. Galambos, L. J. Perkins, S. W. Haney and J. Mandrekas: "Commercial tokamak reactor potential with advanced tokamak operation", Nucl. Fusion, **35**, 5, pp. 551–573 (1995).

[34] Y. Ogawa, N. Inoue and Z. Yoshida: "Parameter optimization of the inductively operated day-long tokamak reactor", Fusion Technol., **24**, pp. 188–199 (1993).

[35] L. A. Artsimovich: "Tokamak devices", Nucl. Fusion, **12**, 2, pp. 215–252 (1972).

[36] H. P. Furth: "Tokamak research", Nucl. Fusion, **15**, pp. 487–534 (1975).

[37] J. Wesson: "Tokamaks", Oxford, Clareandon (1987).

[38] K. Takamura: "Development of system code for tokamak fusion reactor and its application to demo reactor and volumetric neutron source", Bachelor's thesis, Univ.

of Tokyo (1996). (in Japanese).

[39] I. Senda: "Neutron wall loading code, users manual".

[40] T. Watanabe: "Highly accurate calculation of magnetic field produced by body current coils of various shapes", Kakuyugo Kenkyu, **63**, 6, pp. 482–507 (1990). (in Japanese).

[41] H. Ninomiya, A. Kameari and K. Shinya: "A toroidal plasma MHD equilibrium code [EQUCIR version 1]", Technical Report JAERI–M 9127, JAERI (1980). (in Japanese).

[42] K. Shinya and H. Ninomiya: "A MHD equilibrium code [EQUCIR version 2] applicable to up-down asymmetric toroidal plasma", Technical Report JAERI–M 9278, JAERI (1981). (in Japanese).

[43] K. Shinya and S. Nishio: "A toroidal plasma MHD equilibrium code [EQUCIR3]", Technical Report JAERI–M 87–133, JAERI (1987). (in Japanese).

[44] H. Naitou, J. W. V. Dam and D. C. Barnes: "Energetic particle stabilization of ballooning modes in a finite aspect ratio tokamak", Nucl. Fusion, **27**, 5, pp. 765–778 (1987).

[45] H. Naitou and K. Yamazaki: "Beta limit of crescent and bean shaped tokamaks", Nucl. Fusion, **28**, 10, pp. 1751–1764 (1988).

[46] Fujitsu: "EDDYTOR6 eddy current analysis code user's manual" (1983). (in Japanese).

[47] K. Okano, Y. Ogawa and H. Naitou: "Critical beta non-circular tokamak equilibria sustained in steady state be beam driver currents", Nucl. Fusion, **29**, 2, pp. 199–217 (1989).

[48] K. Okano, Y. Ogawa and H. Naitou: "Self-consistent analysis of steady state tokamaks sustained by beam-driven and bootstrap currents", Plasma Phys. and Control. Fusion, **32**, 4, pp. 225–239 (1990).

[49] N. A. Uckan and ITER Physics Group: "ITER Physics Design Guidelines: 1989", ITER Documentation series No. 10, IAEA, Vienna (1990).

[50] R. J. Goldston: "Energy confinement scaling in tokamaks: Some implications of recent experiments with ohmic and strong auxiliary heating", Plasma Phys. and Control. Fusion, **26**, 1A, pp. 87–103 (1984).

[51] R. R. Parker, M. Greenwald, S. C. Luckhardt, E. S. Marmar, M. Porkolab and S. M. Wolfe: "Progress in tokamak research at MIT", Nucl. Fusion, **25**, 99, pp. 1127–1136 (1985).

[52] F. Troyon, R. Gruber, H. Saurenmann, S. Semenzato and S. Succi: "MHD-limits to plasma confinement", Plasma Phys. and Control. Fusion, **26**, 1A, pp. 209–215 (1984).

[53] L. M. Hively: "Convenient computational forms for maxwellian reactivites", Nucl. Fusion, **17**, 4, pp. 873–876 (1977).

[54] N. Inoue, Y. Ogawa, T. Yamamoto, Z. Yoshida, K. Okano and A. Hatayama: "Feasibility study of inductively operated day-long tokamak reactor", Plasma Phys. and Control. Nucl. Fusion Res. 1993, Vol. 3, Vienna, IAEA, pp. 347–353 (1993). (Proc. 14th Int. Conf. Würzburg, 1992).

[55] K. Tomabechi: "ITER: Conceptual design", Plasma Phys. and Control. Nucl. Fusion Res. 1991, Vol. 1, Vienna, IAEA, pp. 217–223 (1991). (Proc. 13th Int. Conf. Washington, 1990).

[56] N. Inoue, Y. Ogawa and Z. Yoshida: "Thermal power regulation system for pulsed fusion reactor", Kakuyugo Kenkyu, **68**, 2, pp. 155–158 (1992).

[57] ITER Joint Central Team: "Parameters of the ITER EDA design", Plasma Phys. and Control. Fusion, **35**, 12, pp. B23–B37 (1993). (Proc. 20th Euro. Conf. Contr. Fus. Plasma Phys., Lisbon, 1993).

[58] the ITER Director: "ITER outline design report", Detail of the ITER Outline Design Report, Vol. 1 (1994). (Proc. 4th. Meeting of the Technical Advisory Committee, San Diego Joint Work Site, 1994).

[59] the ITER Director: "ITER outline design summary", Detail of the ITER Outline Design Report, Vol. 1 (1994). (Proc. 4th. Meeting of the Technical Advisory Committee, San Diego Joint Work Site, 1994).

[60] the ITER Director: "Physics and plasma operation studies", Detail of the ITER Outline Design Report, Vol. 1 (1994). (Proc. 4th. Meeting of the Technical Advisory Committee, San Diego Joint Work Site, 1994).

[61] the ITER Director: "Auxiliary heating and current drive systems", Detail of the ITER Outline Design Report, Vol. 1 (1994). (Proc. 4th. Meeting of the Technical Advisory Committee, San Diego Joint Work Site, 1994).

[62] the ITER Director: "Poloidal field system", Detail of the ITER Outline Design Report, Vol. 1 (1994). (Proc. 4th. Meeting of the Technical Advisory Committee, San Diego Joint Work Site, 1994).

[63] the ITER Director: "Superconducting coils and mechanical structures", Detail of the ITER Outline Design Report, Vol. 2 (1994). (Proc. 4th. Meeting of the Technical Advisory Committee, San Diego Joint Work Site, 1994).

[64] Y. Seki, M. Kikuchi, T. Ando, Y. Ohara, S. Nishio, M. Seki, T. Takizuka, K. Tani,

T. Ozeki, K. Koizumi, Y. Matsuda, M. Azumi, A. Oikawa, H. Madarame, et al.: "The steady state tokamak reactor", Plasma Phys. and Control. Nucl. Fusion Res. 1991, Vol. 1, Vienna, IAEA, pp. 473–485 (1991). (Proc. 13th Int. Conf. Washington, 1990).

[65] M. Kikuchi: "Prospects of a stationary tokamak reactor", Plasma Phys. and Control. Fusion, **35**, 12, pp. B39–B53 (1993). (Proc. 20th Euro. Conf. Contr. Fus. Plasma Phys., Lisbon, 1993).

[66] N. Inoue and Y. Ogawa: "Inductively operated day-long tokamak reactor with high power multiplication factor", Kakuyugo Kenkyu, **67**, 4, pp. 344–351 (1992). (in Japanese).

[67] R. Aymar, V. Chuyanov, M. Huguet, P. R, Y. Simomura, the ITER joint central team and home teams: "ITER Project: A physics and technology experiment", IAEA (1996). (in 16th IAEA Fusion Energy Conference) IAEA-F1-CN-64/01-1, IAEA-F1-CN-64/FP-1.

[68] Y. Ogawa, N. Inoue, T. Yamamoto, K. Okano and J. F. Wang: "DEMO reactor design based on inductively-operated tokamak reactor", 16th Symposium on Fusion Engineering (SOFE-16) (Eds. by G. H. Miley and C. Elliott)IEEE, IEEE, pp. 1190–1193 (1995).

[69] W. M. Stacey: "Extrapolation to a demonstration reactor from the ITER and advanced physics & materials data bases"IAEA (1994). (Proc. 15th Int. Conf. on Plasma Physics and Controlled Nucl. Fusion Research, 1994).

[70] S. O. Dean, C. C. Baker, J. Galambos, Y.-K. M. Peng, et al.: "Pilot plant: A shortened path to fusion power", Plasma Phys. and Control. Nucl. Fusion Res. 1993, Vol. 3, Vienna, IAEA, pp. 355–359 (1993). (Proc. 14th Int. Conf. Würzburg, 1992).

[71] A. Kimura: "Radiation responses of low activation ferritic steels", Kakuyugo Kenkyu, **67**, 6, pp. 497–500 (1992).

[72] T. C. hender, R. Fitzpatrick, A. W. Morris, P. G. Carolan, et al.: "Effect of resonant magnetic perturbations on COMPASS-C tokamak discharges", Nucl. Fusion, **32**, 12, pp. 2091–2117 (1992).

[73] A. Kohyama, M. L. Grossbeck and G. Piatti: "The application of austenitic stainless steels in advanced fusion systems: current limitations and future prospects", J. Nucl. Mater., **191-194**, pp. 37–44 (1992).

[74] S. Shikakura, S. Ukai, Y. Sato, M. Harada, et al.: "Development of advanced austenitic stainless steel for fast reactor core material", J. Atomic Energy. Soc. of Japan, **36**, 5, pp. 441–455 (1994). (in Japanese).

[75] J. F. Wang, T. Yamamoto, T. Amano, Y. Ogawa, K. Okano and N. Inoue: "Conceptual design of a poloidal filed coil system and operation scenario for an inductively operated day-long pulsed tokamak reactor", Fusion Engrg. Des., **29**, pp. 66–77 (1995).

[76] D. E. Post, et al.: "ITER Physics", ITER Documentation series No. 21, IAEA, Vienna (1991).

[77] Fusion Reactor System Laboratory: "Concept study of the steady state tokamak reactor (SSTR)", Technical Report JAERI-M 91-081, JAERI (1991).

[78] Department of Large Tokamak Research: "Quasi steady state fusion experimental reactor (FEQ-Q) Conceptual design report (Standard design FY84)", Technical Report JAERI-M 85-178, JAERI (1985).

[79] Department of Large Tokamak Research: "Conceptual design study of fusion experimental reactor (FER)", Technical Report JAERI-M 86-134, JAERI (1986).

[80] K. Okano and Y. Ogawa: "A necessary condition to achieve $q_0 > 1$ in a long pulse tokamak reactor", J. Plasma Fusion Res., **69**, 8, pp. 968–974 (1993).

[81] N. A. Uckan and J. Sheffield: "Tokamak Start-up", Plenum Press, New York and London (1985). p. 48.

[82] K. Okano, N. Inoue, Y. Ogawa and Z. Yoshida: "Bootstrap currents and its scaling in the non-circular tokamaks", Kakuyugo Kenkyu, **68**, 4, pp. 404–486 (1992). (in Japanese).

[83] F. Troyon, A. Roy, W. A. Cooper, F. Yasseen and A. Tumbull: "Beta limit in tokamaks experimental and computational status", Plasma Phys. and Control. Fusion, **30**, 11, pp. 1597–1609 (1988).

[84] W. A. Houlberg, S. E. Attenberger and L. M. Hively: "Contour analysis of fusion reactor plasma performance", Nucl. Fusion, **22**, 7, pp. 925–945 (1982).

[85] O. Mitarai, A. Hirose and M. Skarsgard: "An alternating current tokamak reactor with ohmic ignition and bootstrap current", Fusion Technol., **20**, pp. 285–294 (1991).

[86] J. P. Christiansen, the JET Team, the DIII-D Research Team, the ASDEX Team, the PDX and PBX-M Team and the JFT-2M Group: "Global energy confinement H-mode database for ITER", Nucl. Fusion, **32**, 2, pp. 291–338 (1992).

[87] J. Mandrekas and W. M. Stacey, Jr: "Evaluation of different control methods for the thermal stability of the international thermonuclear experimental reactor", Fusion Technol., **19**, pp. 57–77 (1991).

[88] D. Anderson, T. Elevant, H. Hamnén, M. Lisak, J. Lorenzen and H. Persson: "Burn

control studies for NET/ITER", FUSION TECHNOLOGY 1990 (Eds. by B. E. Keen, M. Huguet and R. Hemsworth), Elsevier Science Publishers, pp. 1204–1208 (1991).

[89] L. Bromberg, D. R. Cohn and J. L. Fisher: "Regimes of ignited operation", Nucl. Fusion, **19**, 10, pp. 1359–1367 (1979).

[90] L. Bromberg, J. L. Fisher and D. R. Cohn: "Active burn control of nearly ignited plasmas", Nucl. Fusion, **20**, 2, pp. 203–207 (1980).

[91] D. Anderson, T. Elevant, H. Hamnén, M. Lisak and H. Persson: "Studies of fusion burn control", Fusion Technol., **23**, pp. 5–41 (1993).

[92] Y. Murakami, H. Horiike, T. Kuroda, Y. Matsuzaki, Y. Shimomura and M. Sugihara: "Comparison between a steady-state fusion reactor and an inductively driven pulse reactor", Technical Report JAERI–M 92–056, JAERI (1992).

[93] T. Watanabe and S. Sugano: "Particle orbital analysis code manual" (1986). KAKEN–85–002 (in Japanese).

[94] K. Ueda: "Study on the control of the vertical instability and the stabilized reactor structure of tokamak fusion reactor", PhD thesis, University of Tokyo (1990). (in Japanese).

[95] M. R. Perrone and J. A. Wesson: "Stability of axisymmetric modes inJET", Nucl. Fusion, **21**, 7, pp. 871–879 (1981).

[96] Univ. of Nagoya, Plasma Lab. Plan R Design Team: "Fusion reaction plasma experiment device: Technical report [Ⅲ]" (1981). (in Japanese).

[97] L. Bottura, M. Hasegawa, J. Heim, V. Kalinin, H. Katheder, K. koizumi, A. Kostenko, J. R. Miller, N. Mitchell, A. Roshal, J. Schultz, S. S. Shen, L. Summers, E. Tada, K. Yoshida, et al.: "ITER Magnets", ITER Documentation series No. 26, IAEA, Vienna (1991).

[98] K. Okano, N. Inoue, A. Hatayama, Y. Ogawa, T. Yamamoto and Z. Yoshida: "Stability of inductively operated day-long tokamak (IDLT) reactor", Bull. Am. Phys. Soc., **37**, p. 1398 (1992).

[99] O. Mitarai, S. Wolfe, A. Hirose and M. Skarsgard: "Alternating current tokamak reactor with long pulses", Fusion Technol., **15**, pp. 204–213 (1989).

[100] O. Mitarai, S. W. Wolfe, A. Hirose and H. M. Skarsgard: "Stable ac tokamak discharges in the STOR-1M device", Nucl. Fusion, **27**, p. 604 (1987).

[101] B. J. D. Tubbing, N. A. C. Gottardi, B. J. Green, J. A. How, M. Huart, R. Konig, C. G. Lowry, P. J. Lomas, P. Noll, J. J. O'Rourke, P. H. Rebut, D. Stork, A. Tanga, A. Taroni and D. J. Ward: "AC plasma current operation in the JET tokamak", Nucl. Fusion, **32**, 6, pp. 967–972 (1992).

[102] R. Shimada: "Controls of tokamak plasma current and equilibrium with hybrid poloidal field coils", Denki Gakkai Ronbunshi, **A102**, 9, pp. 483–490 (1982). (in Japanese).

[103] J. D. Callen: "Models of plasma confinement and heating in tokamaks", Technical Report UWPR 89–2, Univ. of Wisconsin, Wisconsin (1989). Chap. 4.

[104] K. Tani, T. Takizuka and M. Azumi: "Ripple loss of alpha particles in a tokamak reactor with a non-circular plasma cross-section", Nucl. Fusion, **33**, 6, pp. 903–914 (1993).

[105] T. C. S. for the DIII-D team: "Status and plans for DIII-D", Fusion Technol., **21**, pp. 1332–1339 (1992).

[106] Y. Ogawa, N. Inoue, J. F. Wang, T. Yamamoto, Z. Yoshida, K. Okano, A. Hatayama and T. Amano: "Advanced design of a pulsed tokamak fusion reactor", Plasma Phys. and Control. Nucl. Fusion Res. 1993, Vol. 2, Vienna, IAEA, pp. 803–808 (1993). (Proc. 14th Int. Conf. Würzburg, 1992).

[107] G. L. Jackson, J. Winter, T. S. Taylar, K. H. Burrell, et al.: "Regime of very high confinement in the boronized DIII-D tokamak", Phys. Rev. Lett., **67**, 2, pp. 3098–3101 (1991).

[108] M. C. Zarnstroff, M. G. Bell, M. Bitter, R. J. Goldston, et al.: "Bootstrap current in TFTR", Phys. Rev. Lett., **60**, 13, pp. 1306–1309 (1988).

[109] Y. Ogawa, N. Inoue, Z. Yoshida, T. Yamamoto, K. Okano and A. Hatayama: "Design of a sawtooth free plasma in an inductively-operated pulsed tokamak reactor", J. Plasma Fusion Res., **67**, 10, pp. 1200–1207 (1993).

[110] N. Inoue and Y. Ogawa: "Rationale for conceptual design study of ultra-long-pulse tokamak fusion reactor", J. Plasma Fusion Res., **69**, 4, pp. 313–319 (1993). (in Japanese).

[111] R. Carrera and E. Montalvo: "Fusion ignition experiment", Nucl. Fusion, **30**, 5, pp. 891–901 (1990).

[112] D. A. Ehst, J. N. Brooks, K. Evans and J. Kim: "A comparison of pulsed and steady-state tokamak reactor burn cycles. Part 1: Thermal effects and lifetime limitations", Nuclear Engineering and Design/Fusion, **2**, pp. 305–318 (1985).

[113] "Thermal power stations", Tokyo Electric Power Company Brochure (1992). (in Japanese).

[114] H. Horiike, T. Kuroda, Y. Murakami, M. Sugihara and S. Matsuda: "Comparison between a steady-state fusion reactor and an inductively driven pulse reactor —

study as a power plant—", Technical Report JAERI–M 93–208, JAERI (1993).

[115] P. Rebut, D. Boucher, C. Gormezano, B. E. Keen and M. L. Watkins: "A fusion reactor; continuous or semi-continuous ?", Technical Report JET-P(92)65, JET, UK (1992).

[116] P. Rebut, D. Boucher, D. J. Gambier, B. E. Keen and M. L. Watkins: "The ITER challenge", Technical Report JET-P(92)92, JET, UK (1992).

[117] K. Okano (1995). (private communication).

[118] M. A. Adbou: "A volumetric neutron source for fusion nuclear technology testing and development", Fusion Engrg. Des., **27**, pp. 111–153 (1995).

[119] H. Maekawa and M. A. Adbou: "Summary of experiments and analysis from the JAERI/USDOE collaborative program on fusion blanket neutrons", Fusion Engrg. Des., **28**, pp. 479–491 (1995).

[120] T. E. Shannon, M. J. Rennich, T. Kondo, H. Katsuya, H. Maekawa, et al.: "Conceptual design of the international fusion materials irradiation facility (IFMIF)", IAEA (1996). (in 16th IAEA Fusion Energy Conference) IAEA-F1-CN-64/G2-2.

[121] T. Kawabe, S. Hirayama, Y. Kozaki, K. Yoshikawa, et al.: "The physical and engineering aspects of fusion engineering test facility based on mirror confinement (FEF)", Fusion Technol., **10**, pp. 1102–1110 (1986).

[122] M. Saitoh, Y. Kamata, Z. Yoshida and N. Inoue: "Beam-driven ultra-low-q torus for intense 14MeV neutron source", Kakuyugo Kenkyu, **57**, 4, pp. 241–260 (1987). (in Japanese).

[123] N. Inoue: "Intense neutron source based on ultra-low-q discharge", J. Nucl. Sci. and Technol., **27**, 12, pp. 16–21 (1990).

[124] Y.-K. M. Peng, J. D. Galambos and P. C. Shipe: "Small tokamak for fusion technology testing", Fusion Technol., **21**, pp. 1729–1738 (1992).

[125] H. W. Hendel and D. L. Jassby: "The tokamak as a neutron source", Technical Report PPPL-2656, PPPL (1989).

[126] J. D. Strachan, M. Bitter, A. T. Ramsey, M. C. Zarnstorff, et al.: "High-temperature plasmas in the tokamak fusion test reactor", Phys. Rev. Lett., **58**, 10, pp. 1004–1007 (1987).

[127] M. Abdou, S. Berk, A. Ying, Y. K. M. PENG, S. Sharaft, et al.: "Results of an international study on a high-volume plasma-based neutron source for fusion blanket development", Fusion Technol., **29**, pp. 1–57 (1996).

[128] O. G. Filatov, V. V. Filatov, Y. G. Kuzmim, A. N. Makhankov, et al.: "Some aspects of volumetric neutron source based on tokamak with 'warm' magnet system and inner radiation shield", Fusion Engrg. Des., **31**, pp. 69–82 (1996).

[129] Y. Ogawa, N. Inoue and K. Okano: "A proposal for a material irradiation test reactor based on a steady-state sub-ignited tokamak plasma", Fusion Technol., **26**, pp. 168–178 (1994).

[130] Y. Ogawa, N. Inoue, Z. Yoshida, T. Yamamoto, R. Hiwatari, T. Takemura, K. Tokimatsu, K. Okano, Y. Asada, T. Yoshida, K. Tomabechi, T. Amano, J. Wang and Y. Murakami: "Design of volumetric neutron source based on steady-state tokamak", IAEA (1996). (in 16th IAEA Fusion Energy Conference) IAEA-CN-64/GP-25.

[131] G. Bateman: "MHD Instabilities", The MIT Press, Massachusetts (1980).

[132] J. P. Freidberg: "Ideal Magnetohydrodynamics", Plenum Press, New York and London (1987).

[133] C. Kessel, J. Manickam, G. Rewoldt and W. M. Tang: "Improved plasma performance in tokamaks with negative magnetic shear", Phys. Rev. Lett., **72**, 8, pp. 1212–1215 (1994).

[134] R. J. Goldston: "Physics of the steady-state advanced tokamak", Phys. Plasmas, **3**, 5, pp. 1794–1802 (1996).

[135] J. M. Greene and M. S. Chance: "The second region of stability against ballooning modes", Nucl. Fusion, **21**, 4, pp. 453–464 (1981).

[136] S. A. Sabbagh, M. H. Hughes, M. W. Phillips, et al.: "Transition to the second region of ideal MHD stability", Nucl. Fusion, **29**, 3, pp. 423–435 (1989).

[137] P. Smeulders, L. C. Appel, B. Balet, T. C.Hendel, et al.: "Survey of pellet enhanced performance in JET discharge", Nucl. Fusion, **35**, 2, pp. 225–242 (1995).

[138] E. A. Lazarus, L. L. Lao, T. H. Osborne, T. S. Taylor, et al.: "An optimization of beta in the DIII-D tokamak", Phys. Fluids B, **4**, 11, pp. 3644–3662 (1992).

[139] E. J. Strait, L. L. Lao, M. E. Mauel, B. W. Rice, et al.: "Enhanced confinement and stability in DIII-D discharges with reversed magnetic shear", Phys. Rev. Lett., **75**, 24, pp. 4421–4424 (1995).

[140] H. M. Deitel and P. J. Deitel: "C: HOW TO PROGRAM, 2nd edition", Prentice-Hall (1994).

[141] F. P. Brook, Jr.: "The Mythical Man-Month: essays on software engineering, Anniversary edition", Addison-Wesley (1995). (Japanese translated version).

[142] M. J. LeBrun, T. Tajima, M. G. Gray, G. Furnish and W. Horton: "Toroidal effects on drift wave turbulence", Phys. Fluids B, **5**, 3, pp. 752–773 (1993).

[143] M. J. LeBrun, G. Furnish and T. Tajima: "Large scale gyrokinetic plasma simulation

in a curvilinear metric", 15th Int. Conf. on Numerical Simulation of Plasmas, p. 3A11 (1994).

[144] G. Furnish and M. J. LeBrun: "The generalized tokamak simulation: Design of an object oriented particle code", 15th Int. Conf. on Numerical Simulation of Plasmas, p. 3A27 (1994).

[145] B. J. Cohen, D. C. Barnes, J. M. Dawson, G. W. Hammett, W. W. Lee, et al.: "The numerical tokamak project: simulation of turbulent transport", Comput. Phys. Comm., **87**, pp. 1–15 (1995).

[146] B. Stroustrup: "The C++ Programming Language, 2nd edition", Addison-Wesley Toppan (1993). (Japanese translated version).

[147] M. A. Ellis and B. Stroustrup: "The Annotated C++ Reference Manual", Addison-Wesley Toppan (1992). (Japanese translated version).

[148] B. W. Kernighan and D. M. Ritchie: "The C Programming Language. 2nd edition", Kyoritu Shuppan (1988). (Japanese translated version).

[149] B. Stroustrup: "A better C?", BYTE, pp. 215–216D (1988).

[150] M. Metcalf and J. Reid: "Fortran 90 Explained", Oxford Science Publications (1990). (Japanese translated version).

[151] J. Rumbaugh: "Object-oriented modeling and design", Prentice Hall, Inc. (1991). (Japanese translated version).

[152] B. Stroustrup: "The Design and Evolution of C++", Addison-Wesley (1994).

[153] A. Team: "The H-mode of ASDEX", Nucl. Fusion, **21**, 11, pp. 1959–2040 (1989).

[154] K. Burrell, S. Allen, G. Bramson, et al.: "Confinement physics of H-mode discharges in DIII-D", Plasma Phys. and Control. Fusion, **31**, 10, pp. 1649–1664 (1989).

[155] J. Cordey, D. Muri, S. Neudachin, V. Parail, E. Springmann and A. Taroni: "A numerical simulation of the L-H transition in JET with local and global models of anomalous transport", Nucl. Fusion, **35**, 1, pp. 101–106 (1995).

[156] D. Reiter, G. Wolf and H. Kever: "Burn condition, helium particle confinement and exhaust efficiency", Nucl. Fusion, **30**, 10, pp. 2124–2155 (1990).

[157] O. Mitarai: "The effect of the H-mode power threshold on POPCON in a tokamak reactor" (1995). (Proc. The Japan-US Workshop on Fusion Power Reactors, March 13 – 16, 1995, Kyoto).